




Decreased microglial Wnt/ β -catenin signalling drives microglial pro-inflammatory activation in the developing brain

 Juliette Van Steenwinckel,^{1,2} Anne-Laure Schang,^{1,2,3} Michelle L. Krishnan,⁴ Vincent Degos,^{1,2,5} Andrée Delahaye-Duriez,^{1,6} Cindy Bokobza,^{1,2} Zsolt Csaba,^{1,2} Franck Verdonk,^{7,8} Amélie Montané,^{1,2} Stéphanie Sigaut,^{1,2} Olivier Hennebert,^{1,2,9} Sophie Lebon,^{1,2} Leslie Schwendimann,^{1,2} Tifenn Le Charpentier,^{1,2} Rahma Hassan-Abdi,^{1,2}  Gareth Ball,⁴ Paul Aljabar,⁴ Alka Saxena,¹⁰ Rebecca K. Holloway,¹¹ Walter Birchmeier,¹² Olivier Baud,^{1,2} David Rowitch,¹³ Veronique Miron,¹¹ Fabrice Chretien,^{6,7,14}  Claire Leconte,¹⁵ Valérie C. Besson,¹⁵ Enrico G. Petretto,¹⁶ A. David Edwards,⁴ Henrik Hagberg,^{4,17} Nadia Soussi-Yanicostas,^{1,2} Bobbi Fleiss^{1,2,4,18,*} and Pierre Gressens^{1,2,4,*}

*These authors contributed equally to this work.

Microglia of the developing brain have unique functional properties but how their activation states are regulated is poorly understood. Inflammatory activation of microglia in the still-developing brain of preterm-born infants is associated with permanent neurological sequelae in 9 million infants every year. Investigating the regulators of microglial activation in the developing brain across models of neuroinflammation-mediated injury (mouse, zebrafish) and primary human and mouse microglia we found using analysis of genes and proteins that a reduction in Wnt/ β -catenin signalling is necessary and sufficient to drive a microglial phenotype causing hypomyelination. We validated in a cohort of preterm-born infants that genomic variation in the Wnt pathway is associated with the levels of connectivity found in their brains. Using a Wnt agonist delivered by a blood–brain barrier penetrant microglia-specific targeting nanocarrier we prevented in our animal model the pro-inflammatory microglial activation, white matter injury and behavioural deficits. Collectively, these data validate that the Wnt pathway regulates microglial activation, is critical in the evolution of an important form of human brain injury and is a viable therapeutic target.

- 1 Université de Paris, NeuroDiderot, Inserm, F-75019 Paris, France
- 2 PremUP, F-75006 Paris, France
- 3 UMR CNRS 8638-Chimie Toxicologie Analytique et Cellulaire, Université Paris Descartes, Sorbonne Paris Cité, Faculté de Pharmacie de Paris, 4 Avenue de l'Observatoire, F-75006 Paris, France
- 4 Centre for the Developing Brain, Division of Imaging Sciences and Biomedical Engineering, King's College London, King's Health Partners, St. Thomas' Hospital, London, SE1 7EH, UK
- 5 Department of Anesthesia and Intensive Care, Pitié Salpêtrière Hospital, F-75013 Paris France
- 6 UFR de Santé, Médecine et Biologie Humaine, Université Paris 13, Sorbonne Paris Cité, F-93000 Bobigny, France
- 7 Infection and Epidemiology Department, Human Histopathology and Animal Models Unit, Institut Pasteur, F-75015 Paris, France
- 8 Paris Descartes University, Sorbonne Paris Cité, F-75006 Paris, France
- 9 Conservatoire national des arts et métiers, F-75003 Paris, France
- 10 Genomics Core Facility, NIHR Biomedical Research Centre, Guy's and St Thomas' NHS Foundation Trust, London, SE1 9RT, UK

- 11 MRC Centre for Reproductive Health, The Queen's Medical Research Institute, The University of Edinburgh, Edinburgh, EH16 4TJ, UK
- 12 Cancer Research Program, Max Delbrueck Center for Molecular Medicine in the Helmholtz Society, Berlin-Buch, Germany
- 13 Department of Paediatrics, University of Cambridge, Cambridge, CB2 0QQ, UK
- 14 Laboratoire de Neuropathologie, Centre Hospitalier Sainte Anne, F-75014 Paris, France
- 15 EA4475 – Pharmacologie de la Circulation Cérébrale, Faculté de Pharmacie de Paris, Université Paris Descartes, Sorbonne Paris Cité, F-75006 Paris, France
- 16 Duke-NUS Medical School, 8 College Road 169857, Singapore
- 17 Perinatal Center, Institute of Clinical Sciences and Institute of Neuroscience and Physiology, Sahlgrenska Academy, Gothenburg University, 41390 Gothenburg, Sweden
- 18 School of Health and Biomedical Sciences, RMIT University, Bundoora, 3083, VIC, Australia

Correspondence to: Dr Pierre Gressens

Inserm U1141, Robert Debre Hospital, 48 Blvd Serurier, F-75019 Paris, France

E-mail: pierre.gressens@inserm.fr

Correspondence may also be addressed to: Dr Bobbi Fleiss

RMIT University - Bundoora Campus, Plenty Rd, Bundoora, Victoria, Australia, 3083

E-mail: bobbi.fleiss@rmit.edu.au

Keywords: neuroprotection; 3DNA; neuroinflammation; neonatal encephalopathy; innate immunity

Abbreviations: MACS = magnetically-activated cell sorting; MG/M ϕ = microglia/infiltrating macrophages; OPC = oligodendrocyte progenitor cell; SNP = single nucleotide polymorphism

Introduction

Neuroinflammation is a key pathological mechanism in almost all acute and degenerative diseases in both the adult and in the developing brain (Perry *et al.*, 2010; Hagberg *et al.*, 2012; Hickman *et al.*, 2018). Microglia and infiltrating macrophages (MG/M ϕ) are major contributors to neuroinflammation (Perry *et al.*, 2010). These cells are capable of acquiring numerous complex functional states dependent on the specific nature of an insult or injury, including cytotoxic responses, immune regulation, or injury resolution (Michell-Robinson *et al.*, 2015; Wolf *et al.*, 2017). Limiting the cytotoxic activation of MG/M ϕ while promoting injury resolution represents a rational neuroprotective strategy (Rivest, 2009; Miron *et al.*, 2013) that requires an in-depth understanding of the molecular mechanisms controlling their phenotypes across forms of injury. Understanding of these regulatory mechanisms is increasing at an extraordinary rate for adult disorders. However, microglia do not reach maturity until around the time of birth in humans, or the equivalent developmental time point of approximately postnatal Day 14 in rodents (Butovsky *et al.*, 2014; Bennett *et al.*, 2016; Miyamoto *et al.*, 2016; Krasemann *et al.*, 2017). These microglia, termed pre-microglia (Matcovitch-Natan *et al.*, 2016), have specialized functions in brain development (Thion *et al.*, 2018), but there is a striking paucity of knowledge on the regulators of the microglia phenotype that is relevant to injury/insult to the developing brain.

Preterm birth is the commonest cause of death and disability in children under 5 years of age, exceeding deaths from malaria or pneumonia (Lim *et al.*, 2012). Preterm birth, birth before 37 of 40 weeks of gestation, occurs in

15 million infants yearly; rates are increasing in developed countries (e.g. 7% of all births in the UK; 13% in the US) and we are limited in our predictive and therapeutic options for these vulnerable infants. Up to 60% of infants born preterm will be left with persistent cognitive and neuropsychiatric deficits including autism spectrum, attention-deficit disorders and epilepsy (Wood *et al.*, 2000; Delobel-Ayoub *et al.*, 2009). Insights into the previously poorly understood pathophysiology of preterm birth (Back *et al.*, 2005; Billiards *et al.*, 2008; Delobel-Ayoub *et al.*, 2009; Moore *et al.*, 2012; Verney *et al.*, 2012) have enabled us to design animal models of improved relevance to the constellation of injuries seen in contemporary cohort of infants, collectively called encephalopathy of the premature infant. Encephalopathy of the premature infant involves cerebral white matter injury due to oligodendrocyte maturation blockade and the most severe of injuries widespread neuronal/axonal disease, both of which are linked to the activation of MG/M ϕ (Volpe, 2009b). The strongest predictor for outcomes we currently have in encephalopathy of the premature infant is the severity of white matter/connectivity changes (Woodward *et al.*, 2006; Nosarti *et al.*, 2008, 2014; Spittle *et al.*, 2009). MG/M ϕ activation driving neuroinflammation in preterm-born infants is often caused by exposure to maternal foetal infections or inflammation, such as chorioamnionitis, or post-natal sepsis (Hagberg and Mallard, 2005; Hagberg *et al.*, 2015). Endemic but often clinically silent maternal inflammatory events are considered the chief cause of preterm birth (Wu *et al.*, 2009). As such, exposure to inflammation is both a driver of preterm birth and of brain injury, and further highlighting its importance, increased indices of exposure to inflammation are the

strongest predictor of poor neurological outcome (Hillier *et al.*, 1993; Dammann and Leviton, 2004; Wu *et al.*, 2009).

The Wnt [wingless-type MMTV (mouse mammary tumour virus) integration site] pathways are divided into the canonical Wnt/ β -catenin, the non-canonical Wnt/planar cell polarity (PCP) and the Wnt/calcium pathways. The Wnt pathways have well-studied critical roles in the early developmental events of body axis patterning, and brain cell fate specification, proliferation and migration (Sokol, 2015). Aberrant regulation of canonical WNT/ β -catenin signalling is strongly implicated in the onset and progression of numerous cancers (Zhan *et al.*, 2017). In development, the canonical Wnt pathway has been described as playing a repressive role in the maturation of oligodendrocytes (Shimizu *et al.*, 2005; Feigenson *et al.*, 2009, 2011; Yuen *et al.*, 2014). However, our knowledge has increased and we appreciate that elaborate spatial and temporal regulation of Wnt signalling nudges oligodendrocytes through multiple stages of maturation (Zhao *et al.*, 2016; and reviewed in Guo *et al.*, 2015). Interestingly, Wnt signalling in endothelial cells has also been shown to have important roles in the transmigration of immune cells in the context of multiple sclerosis (Shimizu *et al.*, 2016; Lengfeld *et al.*, 2017). As such, it is clear that the effects of Wnt pathway activation are highly cell and context specific. However, a key regulatory role of the Wnt pathways in the response of MG/M ϕ to injury or insult has not been demonstrated, especially in the developing brain. However, activation of the Frizzled receptors (a family of G protein-coupled receptors) with Wnt ligands has complex effects on some facets of microglia activity *in vitro* (Halleskog *et al.*, 2012; Halleskog and Schulte, 2013). Experimental evidence in other cell types also supports that the Wnt/ β -catenin pathway is involved in aspects of inflammatory signalling, namely, there are links between expression of the inflammatory mediator COX2 (cyclooxygenase-2) and Wnt/ β -catenin in cancer (Buchanan and DuBois, 2006), and evidence that β -catenin regulates at numerous levels the cytokine/pathogen induced activation of NF- κ B (Ma and Hottiger, 2016). As such, in the hunt for a regulator of immature microglia activation state with a view to therapy design the Wnt pathway is an interesting and rationale candidate.

In the present study, we used our mouse model of encephalopathy of prematurity in which we clearly demonstrate a causal link between MG/M ϕ activation and a myelin deficit. This mouse model of encephalopathy of prematurity recapitulates the key neuropathological findings from preterm-born infants, including a myelination deficit, which is the focus of this study (Haynes *et al.*, 2008; Volpe, 2009a; Verney *et al.*, 2012). Using a combination of approaches across species, including human, we reveal for the first time that inhibition of the Wnt/ β -catenin pathway is necessary and sufficient to drive this MG/M ϕ pro-inflammatory phenotypic transformation. We also verified the clinical relevance of the Wnt pathway to anatomical

white matter structure in a cohort of human preterm-born infant brains using an integrated imaging genomics analysis. Finally, we used a novel 3DNA[®] nanocarrier that carries cargo across the blood–brain barrier following non-invasive intraperitoneal administration that then delivers cargo specifically to MG/M ϕ . Using this 3DNA nanocarrier we show that preventing Wnt pathway downregulation specifically in MG/M ϕ reduces the pro-inflammatory MG/M ϕ phenotype, white matter damage and long-term memory deficit in our model of encephalopathy of prematurity.

Altogether, these findings identify the Wnt/ β -catenin pathway as a key regulator of MG/M ϕ activation state across species and a potential target for the treatment of encephalopathy of prematurity and other neuroinflammatory conditions.

Materials and methods

Study approval

Experimental protocols were approved by the institutional guidelines of the Institut National de la Santé et de la Recherche Scientifique (Inserm, France) (Approval 2012-15/676-0079), the Ethics committee, the services of the French ministry in charge of higher education and research according to the directive 2010/63/EU of the European Parliament (Approval #9285-2016090611282348 and #9286-2016090617132750), and met the guidelines for the United States Public Health Service's Policy on Humane Care and Use of Laboratory Animals (NIH, Bethesda, Maryland, USA).

The EPRIME study was reviewed and approved by the National Research Ethics Service, and all infants were studied following written consent from their parents.

For human microglia cell culture, all procedures had ethical approval from Agence de Biomédecine (Approval PFS12-0011). Written informed consent was received from the tissue donor.

Study design

A summary of the independent and total replicates for all experiments, described relative to the figures, is available in Supplementary Table 1.

Nomenclature of microglia phenotype

We adopted nomenclature consistent with our previous work in primary microglia (Chhor *et al.*, 2013) and the work of others (Michell-Robinson *et al.*, 2015) acknowledging that this is a simplification necessary to facilitate description of the data. To simplify, we distinguished three phenotypes according to the mRNA expression levels of markers listed in brackets: pro-inflammatory (*Nos2*, *Ptgs2*, *Cd32*, *Cd86* and *Tnfa*), anti-inflammatory (*Arg1*, *Cd206*, *Lgals3*, *Igf1*, *Il4* and *Il10*) and immunoregulatory (*Il1rn*, *Il4ra*, *Socs3* and *Sphk1*).

Mice

Experiments were performed with male OF1 strain mice pups from adult females purchased from Charles River or transgenic male mice born in our animal facility. See the justification below in animal model section regarding use of male mice only. Transgenic mice B6.129P-Cx3cr1^{tm1Litt}/J (CX3CR1-GFP) mice, B6.129-Ctnnb1^{tm2Kem}/KwJ (β -catenin^{flox}) mice and B6.129P2-Lyz2^{tm1(Cre)Ifo}/J (LysM^{Cre}) mice were purchased from The Jackson Laboratory. CX3CR1-GFP mice express EGFP in monocytes, dendritic cells, natural killer (NK) cells, and brain microglia under control of the endogenous *Cx3cr1* locus. Only heterozygous (Cx3cr1^{GFP/+} and β -catenin ^{Δ /+}) mice were used in this study. Cx3cr1^{GFP/+} are obtained by crossing Cx3cr1^{GFP/GFP} with C57bl6J (wild-type) mice. LysM^{Cre} mice are useful for Cre-lox studies of the myeloid cell lineage. Here, we used it to analyse β -catenin deficit in brain microglia by crossing β -catenin^{flox} with LysM^{Cre} mice. Control mice were obtained by crossing β -catenin^{flox} with C57bl6J (wild-type) mice.

Transgenic fish lines and fish maintenance

Transgenic (pu1::Gal4-UAS-TagRFP) (Sieger *et al.*, 2012) fish were kept at 26.5°C in a 14-h light/10-h dark cycle. Embryos were raised at 28.5°C in E3 solution until 120 h post-fertilization (hpf) for analyses.

Drugs

Mouse cytokines (IL-1 β , IL-4) were purchased from R&D systems. LPS-EB Ultrapure was purchased from InvivoGen. To inhibit the Wnt/ β -catenin pathway, we used XAV939 (Sigma-Aldrich); and to activate it, we used CT99021 (Selleckchem), lithium chloride (Sigma-Aldrich) and L803mts (Tocris). Chelerythrine was purchased from Sigma-Aldrich. To decide on the choice of modulators of Wnt, including considerations for doses and consideration of off target effects we referred to reviews on the subject and previously published works (Fancy *et al.*, 2011, 2014; Keats *et al.*, 2014; Tran and Zheng, 2017). The L803mts peptide and a scrambled peptide (SCR) were purchased conjugated to short oligonucleotide with disulphide bond linker from BioSynthesis then hybridized to Cy3-labelled 3DNA at Genisphere. L803mts was chosen because of its structural properties allowing it to be conjugated to 3DNA and high tolerability have been demonstrated in mice (Kaidanovich-Beilin and Eldar-Finkelman, 2006).

Model of encephalopathy of prematurity induced by systemically driven neuroinflammation

Mice were housed under a 12-h light-dark cycle, had access to food and water *ad libitum* and were weaned into same sex groups at postnatal Day (P)21. Our animal facility has no known pathogens. On P1 pups were sexed and where necessary litters were culled to six to eight (transgenic mice) or 12 (OF1 mice) pups. Assessments of injury and outcomes were made only in male animals and all pups within a litter received

identical treatment to reduce any effects of differing maternal care. All experiments include pups from at least three separate litters. Allocation to phosphate-buffered saline (PBS) or IL-1 β exposure was made in a cage by cage alternating manner. Systemic inflammation was induced by intraperitoneal IL-1 β exposure as described previously (Favrais *et al.*, 2011). Only male mice were used, as only male pups display a myelin deficit following the induction of systemic inflammation to drive neuroinflammation in this paradigm. Specifically, female mice do not have a significant loss of the MBP protein or APC-positive cell number in adulthood like the male mice (P. Gressens, unpublished results). This higher severity of injury in male animals is in accordance with observations of a greater burden of neurological injury in male infants following perinatal insult (Johnston and Hagberg, 2007; Twilhaar *et al.*, 2018). In brief, a 5 μ l volume of PBS containing 10 μ g/kg/injection of recombinant mouse IL-1 β (R&D Systems) or of PBS alone (control) was injected intraperitoneal in male pups twice a day (morning and evening) on P1 to P4 and once in the morning at P5. Animal health was monitored via weight and general visual health assessment and there were no adverse events.

Morphological analysis of microglia

P1 and P3 brains from Cx3Cr1-GFP mice administered PBS or IL-1 β were fixed for 24 h in 4% buffered formalin (QPath, Labonord SAS). Cerebral tissue was sliced along a sagittal plane on a calibrated vibratome (VT1000 S, Leica) into 100- μ m thick free-floating slices. Morphological analysis of microglia was assessed as described previously (Verdonk *et al.*, 2016) using a spinning disk confocal system (Cell Voyager - CV1000) with a UPLSAPO 40 \times /NA 0.9 objective and the use of a 488 nm laser. A mosaic of >100 pictures covering \sim 3.17 mm² of tissue (cortex and white matter) was generated per brain. An automatic image analysis using a custom designed script developed with the AcapellaTM image analysis software (version 2.7, Perkin Elmer Technologies) was carried out to obtain density, cell body area, number of primary, secondary and tertiary processes and the area covered by the microglia processes in 2D. A complexity index was calculated to analyse the morphological modifications induced by IL-1 β .

Neural tissue dissociation and CD11B+ microglia or O4+ oligodendrocyte magnetic-activated cell sorting

At P1, P2, P3, P5 and P10, brains were collected for cell dissociation and CD11B+ cell separation using a magnetic coupled antibody anti-CD11B (MACS Technology), according to the manufacturer's protocol (Miltenyi Biotec) and as described previously (Schang *et al.*, 2014). In brief, mice were intracardially perfused with NaCl 0.9%. After removing the cerebellum and olfactory bulbs, the brains until were pooled ($n = 2-3$ per sample except at P10, $n = 1$) and dissociated using the Neural Tissue Dissociation Kit containing papain and the gentleMACS Octo Dissociator with Heaters. Microglia were enriched using the anti-CD11B (MG)

MicroBeads, pelleted and conserved at -80°C . The purity of the eluted CD11B+ fraction was verified as described previously (Krishnan *et al.*, 2017). At P5 and P10, brains were collected for, O4+ oligodendrocytes cell separation using a magnetic coupled antibody anti-O4 (MACS Technology), according to the manufacturer's protocol (Miltenyi Biotec) and as described previously (Schang *et al.*, 2014).

RNA extraction and quantification of gene expression by real-time qPCR

Total RNA was extracted with the RNeasy[®] mini kit according to the manufacturer's instructions (Qiagen). RNA quality and concentration were assessed by spectrophotometry with the Nanodrop[™] apparatus (ThermoFisher Scientific). Total RNA (500 ng) was subjected to reverse transcription using the iScript[™] cDNA synthesis kit (Bio-Rad). Reverse transcription quantitative polymerase chain reaction (RT-qPCR) was performed in triplicate for each sample using SYBR[®] Green Supermix (Bio-Rad) for 40 cycles with a 2-step program (5 s of denaturation at 95°C and 10 s of annealing at 60°C). Amplification specificity was assessed with a melting curve analysis. Primers were designed using Primer3 plus software (sequences are provided in Supplementary Table 2). Specific mRNA levels were calculated after normalization of the results for each sample with those for *Rpl13a* mRNA (reference gene). The data are presented as relative mRNA units with respect to control group (expressed as fold change over control value).

Immunohistofluorescence

For frozen sections, P1 or P5 mice were intracardially perfused with 4% paraformaldehyde in 0.12 M phosphate buffer solution under isoflurane anaesthesia. Brains were then post-fixed in 4% paraformaldehyde (Sigma-Aldrich) overnight at 4°C . After 2 days in 30% sucrose 0.12 M phosphate buffer solution, brains were frozen at -45°C in isopentane (Sigma-Aldrich) before storage at -80°C until sectioning on a cryostat (14 μm thickness). Immunohistofluorescence was performed as described previously (Miron *et al.*, 2013). Slides were permeabilized and blocked for 1 h and primary antibody was applied overnight at 4°C in a humid chamber. To detect microglia, rabbit antibody to IBA1 (Wako, 1:500) was used. To detect proinflammatory microglia we used mouse antibody to iNOS (BD Biosciences, 610329, 1:100), rat antibody to CD16/CD32 (BD Pharmingen, 553141, 1:500), and rabbit antibody to COX2 (Abcam, Ab15191, 1:500). To detect anti-inflammatory microglia, we used goat antibody to Arginase-1 (ARG1) (Santa Cruz Biotechnology, sc-18355, 1:50), and rabbit antibody to mannose receptor (MR) (Abcam, ab64693, 1:600). To detect microglia and infiltrating macrophage ($M\phi$) rat antibody to CD68 (Abcam, ab53444, 1:100) was used. Fluorescently conjugated secondary antibody to goat IgG (A21432), antibodies to rabbit IgG (A11034, A10042), antibodies to rat IgG (A21434, A11006, A21247) and antibody to mouse IgG (A21042), were applied for 2 h at 20 – 25°C in a humid chamber (1:500, Invitrogen). Following counterstaining with Hoechst, slides were coverslipped with Fluoromount-G (Southern Biotech, Cliniscience). Antibody isotype controls (Sigma-Aldrich) added to sections at the same final concentration as the respective primary antibodies showed little or no

nonspecific staining. All manual cell counts were performed by an investigator who had been blinded to the group allocation of the sample.

In vivo treatments with XAV939, 3DNA L803mts Cy3, and gadolinium

XAV939 (250 μM , 0.5 nmol/injection) or PBS/dimethyl sulphoxide (DMSO) (vehicle) and 3DNA L803mts Cy3 (200 ng/injection) or 3DNA SCR Cy3 (200 ng/injection) (control peptide) were injected into the right ventricle of mice pups at P1 using a 26-G needle linked to a 10 μl Hamilton syringe mounted on a micromanipulator and coupled to a microinjector (Harvard Apparatus; outflow 2 $\mu\text{l}/\text{min}$), 3DNA SCR or L803mts Cy3 were injected 1 h before intraperitoneal injection of PBS or IL-1 β . Three hours after PBS or IL-1 β injection or 4 h after XAV939 or vehicle injection, pups were sacrificed for CD11B+ cell sorting. Chronic treatment with 3DNA L803mts Cy3 were performed by intraperitoneal co-injections of PBS or IL-1 β with 3DNA L803mts Cy3 (500 ng/injection) or 3DNA L803mts Cy3 (500 ng/injection) twice a day between P1 and P3 and once a day at P4 and P5. The effect of this treatment on myelination was analysed at P10, P15 and P30, and behavioural tests were realized in adulthood (2–3 months). To analyse uptake of 3DNA in liver and spleen, one intraperitoneal injection of 3DNA Cy3 (500 ng/injection) with PBS or IL-1 β was performed and animals sacrificed 4 h later. To analyse uptake of 3DNA in brain, animals were sacrificed 4 h after intracerebroventricular injection at P1, and at the end of the intraperitoneal treatment at P5.

Selective depletion of pro-inflammatory microglia in white matter injury was performed using gadolinium chloride (GdCl_3) as described previously (Miron *et al.*, 2013) with slight modifications. Briefly, PBS or gadolinium (200 nmol/injection, Sigma) was injected into the corpus callosum of mouse pups at P1, 1 h before intraperitoneal injections of PBS or IL-1 β using a 26-G needle linked to a 10 μl Hamilton syringe mounted on a micromanipulator and coupled to a microinjector (Harvard apparatus, outflow 2 $\mu\text{l}/\text{min}$). Effect of pro-inflammatory microglia depletion on microglia cell phenotype and myelination was analysed at P15.

Western blotting

Frozen right anterior cortex from P15 mice was homogenized in RIPA Buffer (Sigma-Aldrich) containing protease inhibitors (cOmplete Tablets, Roche) in gentleMACS M tubes using a gentleMACS dissociator (Miltenyi Biotec) as per the manufacturer's instructions. Samples were centrifuged (10 000g, 10 min, 4°C) and the pellets were stored for later use. Equal amounts of protein (25 μg) as determined by BCA protein assays (Sigma-Aldrich), were diluted with Laemmli sample buffer (Bio-Rad) containing 2-mercaptoethanol (Sigma-Aldrich) and then separated in Mini-PROTEAN[®] TGX gels (Any kD[™], Bio-Rad, 80 V for 1 h 50 min). Proteins were then electrotransferred (Trans-Blot[®] Turbo[™], Bio-Rad) onto a 0.2 μm nitrocellulose membrane (Trans-Blot[®] Turbo[™] Transfer Pack, mini, Bio-Rad). The membrane was cut into an upper and lower portion and both were incubated in blocking solution [5% bovine serum albumin, 0.1% Tween 20 in Tris-buffered saline (TBS)] for 1 h. The upper and lower parts

were incubated, respectively, with mouse anti- β -actin (Sigma-Aldrich AC-74, 1:20 000) and rat anti-MBP (Millipore MAB386 1:500) overnight at 4°C in blocking solution. Blots were rinsed with 0.1% Tween 20 in TBS and incubated for 1 h with a HRP-conjugate goat anti-mouse IgG (1:2000; Sigma-Aldrich) or HRP-conjugate goat anti-rat IgG (1:10 000; Invitrogen) in blocking solution. The blots were washed three times with 0.1% Tween 20 in TBS for 5 min. Membranes were processed with the Clarity™ Western ECL substrate (Bio-Rad), and the proteins of interest were investigated with Syngene PXi (Syngene) coupled to acquisition software. The immunoreactivity of four isoforms of MBP was compared with that of actin controls using NIH ImageJ software (<http://rsb.info.nih.gov/ij/>).

Electron microscopy

At P30 mice were transaortically perfused with 20 ml saline followed by 100 ml of ice-cold 2% paraformaldehyde with 2% glutaraldehyde in 0.1 M phosphate buffer, pH 7.4 (PB). Brains were post-fixed overnight in 2% paraformaldehyde at 4°C. Sagittal sections were cut on a vibratome at 70- μ m thickness, post-fixed in 1% glutaraldehyde for 10 min, treated with 1% osmium for 10 min, dehydrated in an ascending series of ethanol, which included 1% uranyl acetate in 70% ethanol. Sections were then treated with propylene oxide, equilibrated overnight in Durcupan™ ACM (Fluka), and flat-embedded on glass slides for 48 h at 60°C. Blocks of the trunk of the corpus callosum (+0.1 mm to -0.1 mm from bregma) close to the midline were cut out from the sections and glued to blank cylinders of resin. Ultrathin sections were cut on a Reichert Ultracut S microtome and collected on Pioloform®-coated single-slot grids. Sections were stained with lead citrate and examined with a Hitachi HT7700 electron microscope (Hitachi High-Technologies) equipped with an AMT XR-41B 4 Megapixel camera (Advanced Microscopy Techniques).

The myelinated axon diameter was measured on cross-sectional axons. For each animal, images were acquired at three dorsoventral positions of three rostrocaudal levels. The thickness of the myelin sheath was assessed by determining the G-ratio (axon diameter/total fibre diameter). An average of 1600 measurements of myelinated axons per animal were performed, using the Fiji version of ImageJ (Schindelin *et al.*, 2012). The axons were pooled by size according to their small (0.2–0.4 μ m), medium (0.4–0.8 μ m) or large (>0.8 μ m) diameter. Results were compared by one-way ANOVA followed by Bonferroni's multiple comparison test, using GraphPad Prism 5.0 (Graph-Pad Software, San Diego, CA, USA). The value of $P < 0.05$ was considered statistically significant.

Behavioural assessments

Actimetry

The horizontal (spontaneous locomotion) and vertical (rearing) activities were individually assessed in transparent activity cages (20 × 10 × 12 cm) with automatic monitoring of photocell beam breaks (Imetronic). An actimetry test was performed at \approx 2 months (Day 65), with recording every 30 min over 23 h, in order to evaluate the effect of IL-1 β and 3DNA treatment intraperitoneal injections on spontaneous locomotor activity,

as modified locomotor activity could lead to biased results from other behavioural tests requiring locomotion.

Open-field test

The open-field test was performed at \approx 2.5 months (Day 80) using a square white open-field apparatus (100 × 100 × 50 cm) made of plastic permeable to infrared light. Distance travelled and time spent in inactivity were recorded by the VideoTrack system (Viewpoint®) during the 9-min test.

Barnes maze test

The Barnes maze test was performed at 3 months (Days 90–105). The maze is a wet, white and circular platform (80-cm diameter), brightly illuminated (400 lx), raised 50 cm above the floor, with 18 holes (4.5 cm) equally spaced around the perimeter. A white hidden escape box (4 × 13 × 7 cm), representing the target, was located under one of the holes. Prior to the test, each mouse was subjected to a habituation trial where the mouse was directly put in the escape box for 30 s.

For the learning phase, the mouse was placed in the centre of the circular maze and allowed to explore the platform and holes for a maximum of 3 min. The distance travelled was recorded using the VideoTrack system (Viewpoint®). Latency to reach the escape box, and number of errors (number of empty holes visited) were manually noted. When the mouse found and entered the escape box, the VideoTrack recording was stopped, and the mouse remained in the escape box for an additional 10 s before returning to its home cage. If the mouse did not enter spontaneously, it was gently put toward the escape box, before returning to its home cage. On the first day of training, mice underwent two trials after the habituation trial; thereafter, three trials were given per day, with a 2-h interval.

On the fifth day of learning the 90-s probe trial was carried out to assess spatial memory performances. The escape box was removed and time spent and distance travelled in each sextant (defined by one of the six parts of the maze, which includes three holes) were recorded. The target zone was defined as the part that contains the target hole and two adjacent holes.

In the long-term trial, 15 days after learning, a new trial, with the escape box, was used to assess long-term retention memory. Escape latency and distance travelled to reach the target were recorded.

Immunohistochemistry

Brains were collected at P15 or P30 and immersed immediately after sacrifice in 4% formaldehyde for 4 days at room temperature, prior to dehydration and paraffin embedding. Section was realized using a microtome. Immunostaining was performed as previously described (Favrais *et al.*, 2011) using mouse antibody to MBP (MAB382, Millipore, France 1:500) or rabbit antibody to OLIG2 (JP18953 IBL 1:200). The intensity of the MBP immunostaining in the anterior corpus callosum and the number of OLIG2+ cells were assessed by a densitometry analysis through NIH ImageJ Software (<http://imagej.nih.gov/ij/>). Optical density was deduced from grey scale standardized to the photomicrograph background. Corpus callosum and/or cingulum were defined as region of interest. One measurement per section (on 40 000 μ m² area) and four sections were analysed in each brain.

Primary mouse microglia culture

Primary mixed glial cell cultures were prepared from the cortices of P1 OF1 mice, as described previously (Chhor *et al.*, 2013). After 14 days, microglia were purified and pelleted via centrifugation and resuspended in Dulbecco's modified Eagle medium/penicillin-streptomycin/10% foetal bovine serum (DMEM/PS/10% FBS) at a concentration of 4×10^5 cells/ml. One or two millilitres per well of cell suspension was plated in 12-well (for qRT-PCR) or 6-well (for ELISA) culture plates, respectively. For immunofluorescence, 250 μ l of cell suspension was plated in μ -Slide 8 Well Glass Bottom chamber slides (Ibidi, BioValley). Post-plating, media was replaced after 1 h. Based on previous work from our lab (Chhor *et al.*, 2013), the day after plating, microglia were exposed for 4 h to DMEM (control) or IL-1 β at 50 ng/ml, IL-4 at 20 ng/ml, diluted in DMEM. For RT-qPCR or ELISA analysis, media were removed and plates frozen at -80°C . For immunofluorescence experiments, cells were fixed at room temperature with 4% paraformaldehyde for 20 min.

Mixed mouse glial and oligodendrocyte progenitor cell cultures

Cortical mixed glial cultures and purified oligodendrocyte progenitor cells (OPCs) were obtained from the cortices of P1 OF1 mice as previously described with slight modification (Shiow *et al.*, 2017). Mixed glial cells were resuspended in MEM-C, which consisted of minimal essential medium (MEM) supplemented with 10% FBS (Gibco), GlutaMAXTM (Gibco), and 1% PS, and plated at 2×10^5 cells/cm² onto T75 flasks for subsequent OPC purification or Ibidi 8-well chamber slides (BioValley) for mixed glial culture treatment. For this purpose, mixed glial cultures were proliferated in MEM-C for 7 days, then maintained for 10–12 days in differentiation medium, which consisted of DMEM-F12 with glutamine (Gibco), N2 (Gibco) and 1% PS. Half of the wells were exposed to IL-1 β (50 ng/ml) and medium was changed every 2–3 days. Alternatively, mixed glial cultures plated onto T75 flasks were maintained for 9–12 days in MEM-C and purified OPC cultures were prepared by a differential shake method (McCarthy and de Vellis, 1980). OPCs were seeded onto Ibidi 8-well chamber slides at a density of 3×10^4 cells/cm² in proliferation medium, which consisted of MACS Neuro Medium with NeuroBrew[®] 21 (Miltenyi Biotec), GlutaMAXTM, 1% PS, FGFb and PDGFA (10 ng/ml each, Sigma-Aldrich). After 72 h, differentiation was induced by FGFb and PDGFA withdrawal and by adding T3 (40 ng/ml, Sigma). Half of the wells were exposed to IL-1 β (50 ng/ml). After 10–12 days (for mixed glial cultures) or 72 h (for OPCs) of IL-1 β , cells were fixed for 20 min with 4% paraformaldehyde.

Primary human microglia culture

Within 1 h of scheduled termination (age 19 and 21 weeks of amenorrhea) brain tissues were collected from two human foetuses without any neuropathological alterations. Brain tissue (4 g) was minced and further mechanically dissociated using a 1 ml micropipettor in Hank's Balanced Salt Solution with Ca²⁺ and Mg²⁺. Using a 70- μ M strainer, a single cell suspension was obtained. MG/M ϕ isolation were obtained using anti-CD11B (MG)

microbeads (MACS Technology), according to the manufacturer's protocol (Miltenyi Biotec), as above. CD11B+ MG/M ϕ were pelleted via centrifugation and resuspended in DMEM/PS/10% FBS at a concentration of 5×10^6 cells/ml. Cells were plated in 12-well plates (1 ml/well) for qRT-PCR analysis. For immunofluorescence analysis, cells were plated in μ -Slide 8 Well Glass Bottom (Ibidi, BioValley). Forty-eight hours after plating, microglia were exposed for 4 h to DMEM (control) or lipopolysaccharide (LPS) 10 ng/ml diluted in DMEM. For RT-qPCR media were removed and plates frozen at -80°C . For immunofluorescence experiments, cells were fixed at room temperature with 4% paraformaldehyde for 20 min.

Immunocytofluorescence

Immunofluorescence staining was performed as described previously (Favrais *et al.*, 2011), using mouse antibody to MBP (MAB382, 1:500; Millipore), rabbit antibody to OLIG2 (18953, 1:500 IBL-America), rabbit antibody to beta-catenin (E247, 1:100; Millipore), rabbit antibody to COX2 (Ab15191, 1:400; Abcam) goat antibody to ARG1 (sc-18354, 1:400; Santa-Cruz) and IL1RA (sc-8482, 1:200, Santa-Cruz). Fluorescently conjugated secondary antibody (all ThermoFisher Scientific) to mouse IgG (A21236), to rabbit IgG (A21206) and to goat IgG (A11055), were applied for 2 h at 20–25 $^\circ\text{C}$ in a humid chamber (1:500, Invitrogen). Slides were coverslipped with Fluoromount-G (Southern Biotech). To analyse MBP labelling, the MBP area was assessed as the percentage of total area above threshold using NIH ImageJ software (<http://imagej.nih.gov/ij/>) and was normalized to the number of Olig2+ cells. Means were expressed as fold change over control condition.

Microarrays and data preprocessing

Gene expression quantification, including RNA extraction and quality assurance, was performed by Miltenyi Biotec on a total of 24 samples of CD11B+ cells and 20 samples of O4+ cells from the brains of mice exposed to IL-1 β or PBS between P1 and P5, and sacrificed at P5 or P10. RNA was extracted and hybridized to Agilent Whole Mouse Genome Oligo Microarrays (8x60K).

Bioinformatic gene co-expression network reconstruction

Expression data

Each cell type and experimental condition was analysed separately, to investigate changes in gene expression over time in response to exposure to IL-1 β or PBS. Expression values for microglia (CD11B+) and oligodendrocytes (O4+) at P5 and P10 were quantile normalized.

Differential expression

Probes showing high variability across time points within each cell type were retained for further analysis (coefficient of variation above 50th centile). Probes showing differential expression between time points were identified using unpaired *t*-tests with Benjamini-Hochberg correction for multiple testing in the Bioconductor multitest package (Gentleman *et al.*, 2004; Schafer and Strimmer, 2005; Opgen-Rhein and Strimmer, 2007), with a false discovery rate threshold (FDR) of 10%.

Network reconstruction

The co-expression network was inferred using Graphical Gaussian Models (GGM), implemented within the software package ‘GeneNet’ (Schafer and Strimmer, 2005) in R (<http://www.r-project.org/>). This analysis computes partial correlations, which are a measure of conditional independence between two genes i.e. the correlation between the expression profiles of two genes after the common effects of all other genes are removed. Correction was made for multiple comparisons by setting the local FDR at $\leq 1\%$. Individual networks were reconstructed for temporally differentially expressed genes for each cell type in each experimental condition (i.e. two cell types \times two conditions). The input for each GGM was a matrix of differentially expressed normalized mRNA transcript levels. The genes in each of these four co-expression networks (Supplementary Fig. 3E) were functionally annotated by calculating significant enrichment of KEGG pathways using the Broad Institute MSigDB database (<http://software.broadinstitute.org/gsea/msigdb/index.jsp>) (Subramanian *et al.*, 2005) (Supplementary Table 3).

Differential expression analysis was performed using the limma package (Smyth, 2004). The mouse datasets were annotated with human Ensembl gene ID using the biomaRt Bioconductor R package (Durinck *et al.*, 2009) and selecting human genes that were ‘one-to-one’ orthologues with mouse genes. We multiplied the adjusted *P*-value (the $-\log_{10}$ of *P*-value) by the log-transformed fold change to generate a gene-level score, which was used as a metric to ‘rank’ genes. Gene set enrichment analysis GSEA (Subramanian *et al.*, 2005) was applied genome-wide to the ranked list of gene scores (reflecting both the significance and the magnitude of expression changes in IL-1 β exposed MG/M ϕ) to test if a group of genes (MSigDB gene sets) occupy higher (or lower) positions in the ranked gene list than what it would be expected by chance. Gene set enrichment scores and significance level of the enrichment (normalized enrichment score, *P*-value, FDR) and enrichment plots were provided in the GSEA output format developed by Broad Institute of MIT and Harvard (permutations = 10 000). The GSEA was carried out accounting for the direction of IL-1 β effect, i.e. considering whether a gene is up- or downregulated under IL-1 β exposure at P5 and P10.

Wnt/ β -catenin pathway modulation in primary microglia

Microglia transfection was realized using negative control siRNA or siRNA *Axin2* (ON TARGET Plus Control Pool and ON TARGET Plus mouse *Axin2*-06, Thermo Scientific, Dharmacon) at a final concentration of 30 μ M. Transfection was realized using the MACSfectinTM transfection reagent (Miltenyi Biotec) in a mixture of Opti-MEMTM and DMEM mediums for 48 h prior to IL-1 β stimulation. *Axin2* mRNA knockdown was evaluated by qRT-PCR. XAV939 and CT99021 (1 μ M) or PBS/DMSO (vehicle) were added to media 30 min before DMEM (control) or IL-1 β (50 ng/ml) treatments.

PSer45 β -catenin and β -catenin quantification by ELISA

Quantification of PSer45 β -catenin and β -catenin by enzyme-linked immunosorbent assay (ELISA) was realized using β -catenin pSer45 + Total PhosphoTracer ELISA Kit (ab119656,

Abcam) for primary microglia or β -catenin ELISA Kit (ab1205704, Abcam) for magnetically-activated cell sorted (MACS) cells. Briefly, cell lysates were obtained using lysis buffer of the kit. Total protein level was quantified using BCA method [Bicinchoninic Acid Solution and Copper (II) Sulfate Solution from Sigma]. The ELISA was carried out according to the manufacturer’s instruction. Quantification of PSer45 β -catenin is a ratio PSer45 β -catenin/total β -catenin. Total β -catenin was normalized using total protein level. Total β -catenin data are expressed as fold change over control values.

Wnt/ β -catenin pathway modulation in Zebrafish

Microglia were visualized using pu1::Gal4-UAS::TagRFP. Zebrafish embryos aged 72 hpf were used for LPS microinjection (5 ng/injection) in hindbrain. The Wnt/ β -catenin pathway was modulated by adding LiCl (80 mM), XAV939 (5 μ M), CT99021 (3 μ M) in E3 solution. Fluorescently-labelled embryos were imaged using a microscope equipped with an ApoTome system (Zeiss) fitted with an AxioCam MRm camera (Zeiss) controlled by the Axiovision software. The thickness of the *z*-stacks was always between 2.5 and 3 μ m. Fluorescence intensity was quantified by NIH ImageJ software (<http://imagej.nih.gov/ij/>) on greyscale images.

Preterm infant cohort

Preterm infants were recruited as part of the EPRIME [Evaluation of Magnetic Resonance (MR) Imaging to Predict Neurodevelopmental Impairment in Preterm Infants] study and were imaged at term-equivalent age over a 3-year period (2010–13) at a single centre. The EPRIME study was reviewed and approved by the National Research Ethics Service, and all infants were studied following written consent from their parents. A total of 290 infants (gestational age 23.57 to 32.86 weeks, median 30 weeks) were scanned at term-equivalent age (38.29 to 58.28 weeks); additional cohort details are available in Supplementary Table 4. Pulse oximetry, temperature, and heart rate were monitored throughout the period of image acquisition; ear protection in the form of silicone-based putty placed in the external ear (President Putty, Coltene) and Mini-muffs (Natus Medical Inc.) were used for each infant.

Image acquisition

MRI was performed on a Philips 3-T system using an 8-channel phased array head coil. The 3D-MPRAGE and high-resolution T₂-weighted fast spin echo images were obtained before diffusion tensor imaging (DTI). Single-shot EPI DTI was acquired in the transverse plane in 32 non-collinear directions using the following parameters: repetition time: 8000 ms; echo time: 49 ms; slice thickness: 2 mm; field of view: 224 mm; matrix: 128 \times 128 (voxel size: 1.75 \times 1.75 \times 2 mm³); *b*-value: 750 s/mm². Data were acquired with a SENSE factor of 2.

Data selection and quality control

The T₂-weighted MRI anatomical scans were reviewed to exclude subjects with extensive brain abnormalities, major focal destructive parenchymal lesions, multiple punctate white

matter lesions or white matter cysts, as these infants represent a heterogeneous minority (1–3%) with different underlying biology and clinical features to the general preterm population (Hamrick *et al.*, 2004; van Haastert *et al.*, 2011). All MRIs were assessed for the presence of image artefacts (inferior-temporal signal dropout, aliasing, field inhomogeneity, etc.) and severe motion (for head-motion criteria see below). All exclusion criteria were designed so as not to bias the study but preserve the full spectrum of clinical heterogeneity typical of a preterm born population. Two hundred and ninety infants had images suitable for tractography and associated genetic information.

DTI analysis was performed using FMRIB's Diffusion Toolbox (FDT v2.0). Images were registered to their non-diffusion weighted (*b*₀) image and corrected for differences in spatial distortion due to eddy currents. Non-brain tissue was removed using the brain extraction tool (BET) (Smith, 2002). Diffusion tensors were calculated voxel-wise, using a simple least-squares fit of the tensor model to the diffusion data. From this, the tensor eigenvalues and fractional anisotropy maps were calculated.

Probabilistic tractography

Regions of interest for seeding tracts were obtained by segmentation of the brain based on a 90-node anatomical neonatal atlas (Shi *et al.*, 2011), and the resulting segmentations were registered to the diffusion space using a custom neonatal pipeline (Ball *et al.*, 2010). Tractography was performed on DTI data using a modified probabilistic tractography that estimates diffusive transfer between voxels (Robinson *et al.*, 2008) using cortico-cortical connections only. A weighted adjacency matrix of brain regions was produced for each infant: self-connections along the diagonal were removed; symmetry was enforced; and the redundant lower triangle removed. The edges of these connectivity graphs were vectorized by concatenating the rows for each individual connectivity matrix, and appending them to form a single matrix of *n* individuals by *p* edges. Each phenotype matrix was adjusted for major covariates (post-menstrual age at scan and at birth) and reduced to its first principal component.

Genome-wide genotyping

Saliva samples from 290 preterm infants with imaging data were collected using Oragene DNA OG-250 kits (DNAGenotek Inc.) and genotyped on Illumina HumanOmniExpress-24 v1.1 chip. Filtering was carried out using PLINK (<https://www.cog-genomics.org/plink2>). All individuals had missing call frequency < 0.1. Single nucleotide polymorphisms (SNPs) with Hardy-Weinberg equilibrium exact test $P \geq 1 \times 10^{-6}$, minor allele frequency ≥ 0.01 and genotyping rate > 0.99 were retained for analysis. After these filtering steps, 659 674 SNPs remained. Additional details of these analyses and the STREGA details are found in the original description of the cohort (Boardman *et al.*, 2014).

Preterm infant imaging genomics analysis of the Wnt pathway

A list of all genes in the *WNT* signalling pathway (entry hsa04310) in the Kyoto Encyclopaedia of Genes and

Genomes (KEGG) was used as a gene-set of interest ($n = 141$ genes). Gene-set analysis was carried out with the Joint Association of Genetic Variants (JAG) tool (Lips *et al.*, 2012, 2015) to test the joint effect of all SNPs located in the *Wnt* pathway. This procedure consists of three parts: (i) SNP to gene annotation; (ii) self-contained testing (i.e. association); and (iii) competitive testing (i.e. enrichment). An enriched pathway can be defined as one whose genes are more strongly associated with the phenotype than those genes outside the pathway. Phenotype permutation is used to evaluate gene-set significance, implicitly controlling for linkage disequilibrium, sample size, gene size, number of SNPs per gene, and number of genes in a gene-set. This will result in a *P*-value (with a traditional significance threshold < 0.05) if there is an enrichment for variants associated with the phenotype within the gene-set of interest compared to random matched gene-sets.

Following SNP-gene mapping, genes in the *WNT*-set were tested for association with the original phenotype (query data), and this was repeated with 1000 permutations of the phenotype (self-contained/association test). This association testing tests the null hypothesis that no pathway genes are associated with the phenotype and combines the individual gene association *P*-values into a single *P*-value for the entire pathway. The competitive/enrichment test was then done to test the null hypothesis that the pathway genes are no more associated with the phenotype than 300 randomly drawn non-pathway gene-sets, with 1000 phenotype permutations. The association analysis was repeated gene-by-gene within the *WNT* gene-set to investigate which members of the gene-set might be predominantly contributing to the collective signal.

Statistical analysis

No statistical methods were used to predetermine sample sizes, but these were similar to those generally used in the field. Data are expressed as the mean values \pm standard error of the mean (SEM). Data were first tested for normality using the Kolmogorov-Smirnov normality test for $n = 5-7$ and D'Agostino and Pearson omnibus normality test for $n > 7$. *F*-test (single comparisons) or Bartlett's test (multiple comparison) for ANOVA was used. Multiple comparisons in the same dataset were analysed by one-way ANOVA with Newman-Keuls *post hoc* test, two-way ANOVA with Bonferroni *post hoc* or Kruskal-Wallis test with Dunns *post hoc*. Single comparisons to control were made using two-tailed Student's *t*-test or Mann-Whitney test. $P < 0.05$ was considered to be statistically significant. For the Barnes maze probe trial, univariate *t*-test was performed to compare the per cent time spent in the target sextant to the theoretical value 16.67% (i.e. when the mouse spent equal time within each sextant). Data handling and statistical processing was performed using Microsoft Excel and GraphPad Prism Software.

Data availability

All new data are available from the authors on request, subject to ethical restrictions related to the human studies.

Results

Microglial activation drives hypomyelination in our model of encephalopathy of the premature infant

To understand the mechanisms underpinning encephalopathy of the premature infant in contemporaneous cohorts we previously set up a model mimicking its neuropathological, behavioural and imaging phenotypes (Favrais *et al.*, 2011; Krishnan *et al.*, 2017). Of note, the neuropathological similarities between our model and clinical studies include MG/M ϕ activation and hypomyelination due to the maturation blockade of oligodendrocytes but limited cell death (Billiards *et al.*, 2008; Verney *et al.*, 2010, 2012). Specifically, intraperitoneal injections of IL-1 β (10 μ g/kg) were administered to mouse pups twice daily on P1–4 and once at P5 (Fig. 1A). P1–P5 in the mouse is a developmental period roughly corresponding to 22–32 weeks of human pregnancy (Marret *et al.*, 1995) and this is the greatest period of vulnerability for white matter damage in preterm-born infants. Exposure to systemic IL-1 β recapitulates the systemic inflammatory insult of maternal/foetal infections. Specifically, intraperitoneal IL-1 β injection causes a complex systemic response including increased blood levels of IL-6, TNF α and IL-1 β (Favrais *et al.*, 2011) that lead to neuroinflammatory responses including microglial activation with increased cytokines and chemokines (Krishnan *et al.*, 2017; Shioh *et al.*, 2017). The eventual outcome is an oligodendrocyte maturation delay that can be observed specifically as an increase in the numbers of NG2+ and PDGFR α + OPC/pre-oligodendrocyte populations, decreased expression of MBP, MAG and MOG, and altered axonal myelination into adulthood (Favrais *et al.*, 2011; Schang *et al.*, 2014; Shioh *et al.*, 2017) associated with cognitive dysfunction (Favrais *et al.*, 2011). In this study, we verified a direct causal link between MG/M ϕ activation and neuropathology in our model by selectively killing pro-inflammatory MG/M ϕ and observing a reduction in myelin injury. Specifically, we used an intracerebral injection of GdCl₃, which kills pro-inflammatory MG/M ϕ via competitive inhibition of calcium mobilization and damage to the plasma membrane. We validated *in vivo* that this approach is effective at reducing the numbers of pro-inflammatory microglia in the developing brain, and it has previously been validated *in vivo* in adult models of injury (Fulci *et al.*, 2007; Miron *et al.*, 2013; Du *et al.*, 2014). We chose this approach and not ablation of microglia with a tamoxifen-driven transgenic or other pharmacological approach (i.e. PLX3397, ganciclovir) as our studies target maturing oligodendrocytes (as found in the preterm infant brain) that are present from P1. These conditional and pharmacological depletion methods cannot practically be made effective at

P1 and this window of development is key to this model. Also, embryonic depletion of microglia itself alters brain development (Squarzoni *et al.*, 2014) in ways that would alter our experimental paradigm. GdCl₃ (200 nmol) was injected into the corpus callosum of P1 mice prior to intraperitoneal injection of IL-1 β or PBS. In the corpus callosum at P3, after 72 h of exposure to systemic inflammation, immunohistological analysis revealed that the majority of MG/M ϕ were IBA1+/COX2+ and the numbers of these cells was reduced by ~50% by GdCl₃ (Fig. 1B and C). This GdCl₃-mediated reduction in MG/M ϕ prevented the typical loss of MBP in the corpus callosum at P30 (Fig. 1D and E), but OLIG2 was not altered by exposure to systemic inflammation, as reported previously (Favrais *et al.*, 2011) or GdCl₃ (Fig. 1F and G). A link between microglial activation and hypomyelination can also be recapitulated with inflammatory activation of mixed glial cultures containing OPCs, microglia and astrocytes. In these *in vitro* conditions, there is reduced MBP+ cell density, without affecting the total number of oligodendrocytes (Fig. 1H). Exposure of pure OPC cultures (in the absence of microglia or astrocytes) to an inflammatory stimulant, IL-1 β , did not cause hypomyelination (data not shown). Altogether, these results validate in our model a causal link between MG/M ϕ activation and the hypomyelination that is a hallmark of encephalopathy of prematurity.

Microglial activation is persistent with specific temporal patterns in our model of encephalopathy of the preterm infant

We comprehensively characterized the morphology, gene and protein expression of MG/M ϕ over time in our model to assess the relationship between activation states and injury. Our morphological analysis of GFP+ MG/M ϕ from CX3CR1^{GFP/+} mice revealed a moderate but significant reduction of complexity (arborization) at P3 when comparing MG/M ϕ from IL-1 β versus PBS-injected animals, but no difference in process length or density, cell body area, numbers of primary, secondary and tertiary processes, or the area covered by the microglia processes in 2D (Fig. 2A and B). Cell morphology was measured at 3 h after the first inflammatory challenge (at P1) and at P3 when animals had been exposed to >48 h of systemic inflammation driven neuroinflammation in vibratome-cut sections using a custom designed script developed with the AcapellaTM image analysis (Verdonk *et al.*, 2016).

We further studied MG/M ϕ activation using expression analysis of 16 genes and six protein markers previously associated with polarized expression states (Chhor *et al.*, 2013; Miron *et al.*, 2013) at five time points. Gene expression analysis was performed in CD11B+ cells isolated by MACS (Miltenyi Biotec) from PBS- or IL-1 β -exposed mice as per our previous studies (Chhor *et al.*, 2017; Krishnan *et al.*, 2017; Shioh *et al.*, 2017). Prior FACS analysis has

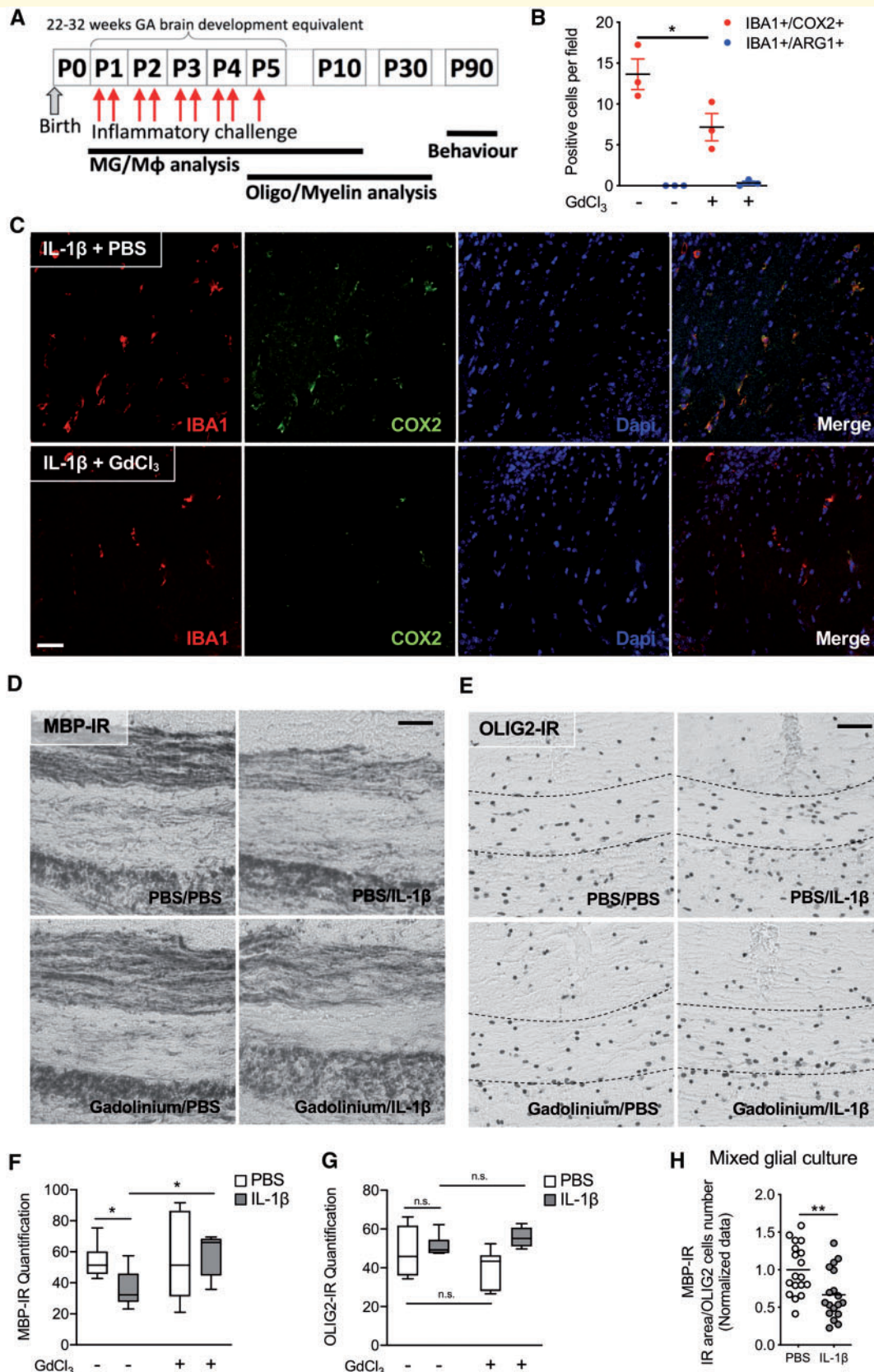


Figure 1 MG/M ϕ are required to induce hypomyelination in our model of encephalopathy of prematurity. **(A)** Schematic of the experimental paradigm for modelling systemic inflammation-associated encephalopathy of prematurity and the timing of analysis; MG/M ϕ and oligodendrocytes (Oligo). Of note, experiments needed to be performed between P1 and P5 as this is when oligodendrocyte maturation in the mouse matches that found in vulnerable preterm-born infants, those born between 22 and 32 weeks gestation (GA). **(B–H)** Demonstration that

(continued)

demonstrated that the ratio of microglia to other CD11B+ cells in this isolate is greater than 50 to 1 (Krishnan *et al.*, 2017). Nevertheless, because we cannot exclude the presence of M ϕ completely we use MG/M ϕ as the descriptor for these cell isolates. Also, the purity of the MACS isolation was confirmed as >95% CD11B+ MG/M ϕ by fluorescence-activated cell sorting (FACS) and qRT-PCR, also as previously (Schang *et al.*, 2014; Krishnan *et al.*, 2017). Quantitative RT-PCR-based gene expression analysis (Fig. 2C) and immunofluorescence (Supplementary Fig. 1A–D) showed that systemic exposure to IL-1 β induced a robust pro-inflammatory MG/M ϕ activation state at P1, only 3 h following the first injection of IL-1 β . Specifically, five of six markers of a pro-inflammatory state were significantly increased including *Il6* increased by 20-fold, and a 5-fold increases in *Ptgs2* and *Nos2*, all $P < 0.001$. Of note, *Ptgs2* and *Nos2* remained elevated for 5 days, but *Il6* and *Tnfa* were returned to normal by P3. There was a similar robust increase in markers of immune-regulation at P1 as all four markers examined were increased including an 8-fold increase in *Socs3* and >10-fold increase for *Sphk1* and *Il1rn*, all $P < 0.001$. Expression of markers associated with an anti-inflammatory activation state were the most effected in animals exposed to systemic IL-1 β exposure at P2 and P3, which is 48 or 72 h after the start of IL-1 β injections. These findings of a temporal change in MG/M ϕ activation profiles were corroborated with immunohistological analysis of protein levels (Supplementary Fig. 1A–D).

By combining our observations of morphology, gene and protein changes in MG/M ϕ after systemic IL-1 β exposure we have characterized a persistent state of activation responsible for injury to the developing white matter.

The Wnt pathway is comprehensively downregulated in activated microglia *in vivo* and *in vitro*

In mouse pups exposed to systemic IL-1 β we have characterized a persistent activation of microglia between P1 and until at least P5, which induces a partial blockade of OPC maturation and subsequently hypomyelination (Favrais *et al.*, 2011). Using gene and predicted protein network-based analysis, we sought to identify molecular pathways regulating this MG/M ϕ activation driving OPC injury. We hypothesized that the best time to pick-up the potential disrupting regulator pathways specific to developing

microglia was P5, when microglia are activated and when the first effects of OPCs have been observed, and P10, when microglia activation is apparently resolved but injury to OPCs is well established. As such, we undertook genome-wide transcriptomics analysis of MG/M ϕ (CD11B+) and OPCs (O4+) MACSed at P5 and P10 from the brains of mice exposed to IL-1 β or PBS. The purity of the O4+ MACS isolation was verified with qPCR (Schang *et al.*, 2014) as outlined for CD11B fractions above. Genes showing differential expression between time points, P5 and P10, were identified for each cell-type, MG/M ϕ (CD11B+) or OPCs (O4+), within each condition, IL-1 β or PBS. Gene co-expression networks were inferred for each of the four sets of differentially expressed genes using GGMs (Oppenheim and Strimmer, 2007). GGMs use partial correlations to infer significant co-expression relationships. We applied an FDR of <1% between any microarray probe pair in each of the four sets of differentially expressed genes sets previously identified: PBS-OPC, IL-1 β -OPC, PBS-MG/M ϕ and IL-1 β -MG/M ϕ . These four co-expression networks were found to exhibit unique topologies and functional annotations (Supplementary Fig. 2A, B and Supplementary Tables 3 and 5). Compared to the three other conditions networks, the IL-1 β exposed MG/M ϕ co-expression network was the most highly interconnected and the densest indicating a strong co-regulation of gene expression under this condition (Supplementary Fig. 2A and B). Biological pathway analysis using the Broad Institute MsigDB database (Subramanian *et al.*, 2005) indicated enrichment for Wnt signalling pathway genes within the IL-1 β exposed MG/M ϕ network (FDR = 8.5×10^{-7} ; Fig. 3A and Supplementary Table 3). Because of the proposed importance of the Wnt pathway in OPC maturation (Fancy *et al.*, 2009) we undertook a specific analysis of data from the O4+ OPCs from mice subjected to systemic exposure to IL-1 β . Analysis of microarray data from the O4+ OPCs did not show any significant enrichment for Wnt signalling genes in the gene co-expression response (Supplementary Table 3). These data highlight two important facts about Wnt dysregulation: (i) that Wnt dysregulation is likely not a mechanism that directly effects oligodendrocytes in this model; and (ii) that changes in Wnt are not simply ubiquitous in the developing CNS in response to inflammation. Returning to the analysis of MG/M ϕ , to highlight the directionality of the data, we looked for enrichments for Wnt

Figure 1 Continued

oligodendrocyte injury in our model is dependent on activated MG/M ϕ by inducing cell death in these cells. Specifically, PBS or IL-1 β exposed mice were injected in the corpus callosum with vehicle (PBS) or GdCl₃; 200 nmol at P1. (B) Scatter plot showing the reduced numbers of pro-inflammatory (IBA1 + /COX2+) and stable numbers of anti-inflammatory (IBA1 + /ARG1+) MG/M ϕ in corpus callosum at P3 (mean \pm SEM, Mann-Whitney test, * $P < 0.05$, $n = 3$ /group) as illustrated by representative images in C of IBA1-immunoreactivity (IR), COX2-IR and DAPI (scale bar = 100 μ m). Following GdCl₃ treatment, representative images showing MBP-IR (D) and OLIG2-IR (E) (scale bars = 20 μ m) in the corpus callosum at P15, and min to max box and whisker plots of the quantification of MBP-IR (F) and OLIG2-IR (G) (Mann-Whitney test, * $P < 0.05$, $n = 5$ –6/group). The requirement for the presence of MG/M ϕ to illicit demyelination was also verified *in vitro* in mixed glial cultures in H, scatter plots of MBP-IR normalized by OLIG2+ cell number in mixed cell culture (mean, Mann-Whitney test ** $P < 0.01$ and $n = 18$ /group).

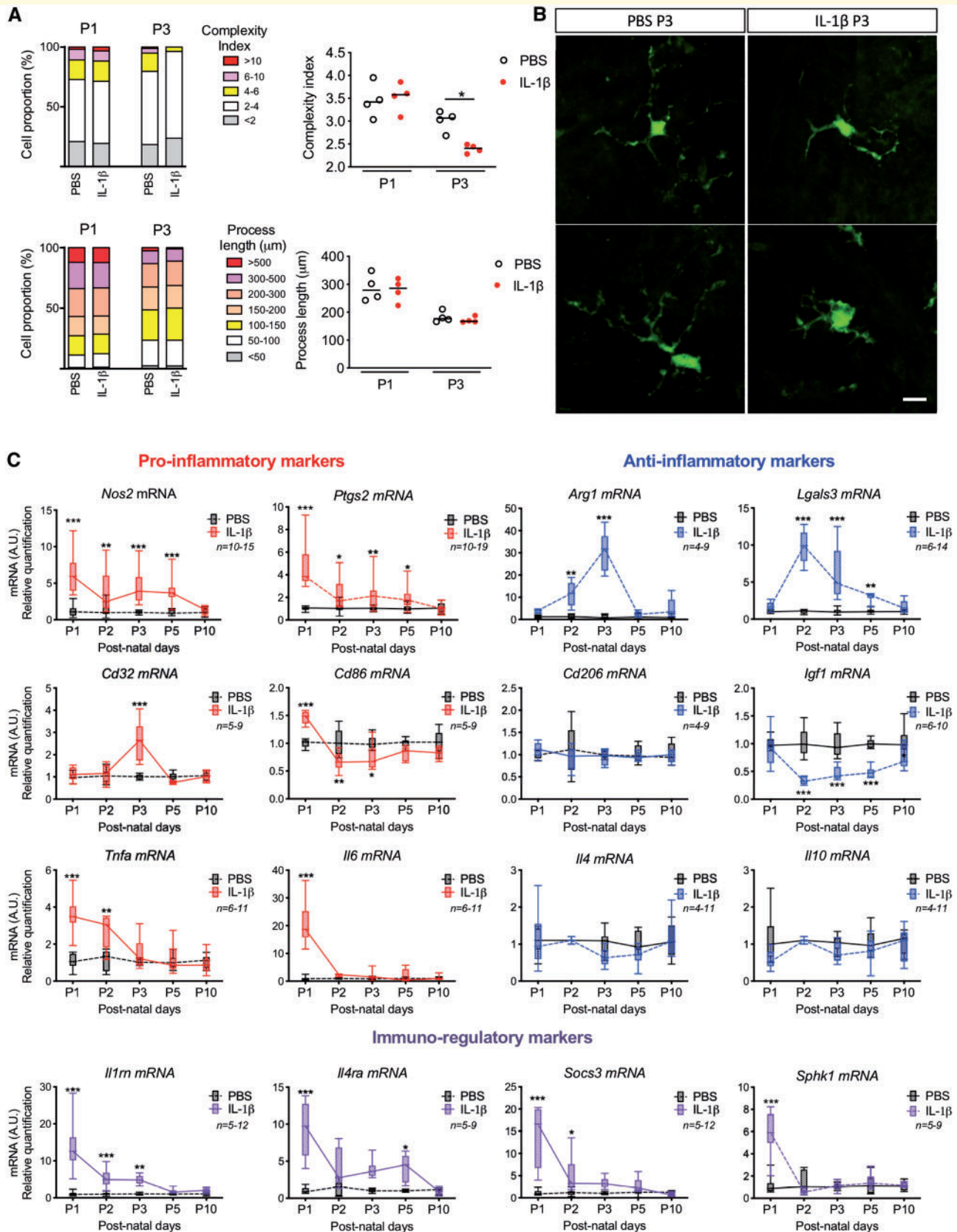


Figure 2 MG/M ϕ have a subtly altered morphology and bi-phase alterations to phenotype in our model of encephalopathy of prematurity. **(A)** Quantification of the complexity of MG/M ϕ ramifications and process length in CX3CR1GFP/+ mice exposed by intraperitoneal injection of PBS or IL-1 β for 3 h (P1) or for 48 h (P3). The panel shows the proportion (%) and the scatter plots of the complexity index and the process length MG/M ϕ (mean, Mann-Whitney test, * $P < 0.05$, $n = 4$ /group). **(B)** Representative images of IL-1 β induced decrease in the

(continued)

signalling pathway sets among the genes significantly down-regulated by IL-1 β exposure at P5 and P10 (Supplementary Table 6, see ‘Materials and methods’ section). The known interactions among the Wnt pathway genes plus predicted interactors were then retrieved from an extensive set of functional association data by the GeneMania tool (Warde-Farley *et al.*, 2010) and we present this sub-network in Fig. 3B. We annotated this figure to highlight that the vast majority of targets predicted to interact in this model have downregulated expression. Finally, qualitative gene profiling with qRT-PCR in CD11B+ MG/M ϕ confirmed the down-regulation of mRNA expression for numerous Wnt pathway members including multiple Frizzled receptors, *Lef1* and *Ctmb1* in MG/M ϕ from IL-1 β -exposed mice (Fig. 3C). The downregulation of *Ctmb1* mRNA was also accompanied by a significant decrease in the expression of β -catenin protein in CD11B+ MG/M ϕ at P3 corresponding to the time point when the greatest morphological changes and pro-inflammatory gene activation is observed (Fig. 3D).

To extend this *ex vivo* CD11B+ cell data and set up an *in vitro* model for further study, qRT-PCR and immunofluorescence analysis of mouse primary cultured microglia were undertaken. The cultures are >97% pure for microglia as validated with immunohistochemistry and qRT-PCR, as previously reported (Chhor *et al.*, 2013). Exposure of microglia to IL-1 β *in vitro* induces a similar pro-inflammatory phenotype as is found in MG/M ϕ from mice exposed to systemic IL-1 β (Supplementary Fig. 3A and B, *cf.* data in Fig. 2C). Furthermore, we observed a similar downregulation of Wnt pathway members including mRNA encoding Fzd receptors, *Ctmb1* and *Tcf1* (Supplementary Fig. 3C). Inducing a pro-inflammatory activation in microglia *in vitro* also induced an upregulation of mRNA encoding *Axin1* and *Axin2*, two specific inhibitors of β -catenin nuclear translocation (Supplementary Fig. 3C) and reduced the protein levels for β -catenin as assessed with immunofluorescence (Supplementary Fig. 3D), and ELISA (Supplementary Fig. 3E). There was no significant change in the ratio of phosphorylated (Pser45) β -catenin to β -catenin also assessed with ELISA (Supplementary Fig. 3E). In contrast, IL-4, a classic anti-inflammatory stimulus, increased Wnt/ β -catenin activation as indicated by strongly increased *Lef1* mRNA and decreased the Pser45 β -catenin/ β -catenin ratio as measured by ELISA (Supplementary Fig. 3F and G).

Altogether these data demonstrate that a pro-inflammatory MG/M ϕ phenotype is associated with a robust and comprehensive downregulation of the gene and protein expression of members of the Wnt/ β -catenin signalling pathway *in vivo* and *in vitro*.

Wnt/ β -catenin pathway activity negatively correlates with pro-inflammatory microglia activation *in vitro*

We next sought to determine if Wnt/ β -catenin pathway modulation alone is sufficient to drive phenotypic changes in microglia *in vitro*. Pharmacological inhibition of the Wnt/ β -catenin pathway *in vitro* with XAV939, a tankyrase inhibitor that stabilizes the Wnt/ β -catenin pathway inhibitor AXIN2 (Fancy *et al.*, 2011), was sufficient to promote a pro-inflammatory phenotype, mimicking the effects of IL-1 β (Fig. 3E). Conversely, the IL-1 β -induced pro-inflammatory microglia phenotype was blocked by activating the Wnt pathway using siRNAs against AXIN2 (Fig. 3F; validation of siRNA efficacy is presented in Supplementary Fig. 3H) or a pharmacological inhibitor of GSK3 β that phosphorylates and inactivates β -catenin, CT99021 (Ring *et al.*, 2003) (Fig. 3G). As expected, we verified with ELISA that the Pser45 β -catenin/ β -catenin ratio was increased with XAV939, and decreased with *Axin2* siRNA and CT99021 (Fig. 3H). In contrast, we tested in PBS and IL-1 β -exposed primary microglia a non-isoform specific block of PKC signalling with chelerythrine. Chelerythrine targets the non-canonical Wnt pathways and exposure of doses at 1–3 μ M had no effect on microglia activation via qRT-PCR (Supplementary Fig. 4). It is worth noting that all pharmacological approaches are liable to off target effects, but altogether the multiple compounds, and genetic targeting create a cohesive link to the Wnt canonical pathway as being key to microglia activation.

Altogether, these data verify in pure cultures of primary microglia that modulating the Wnt/ β -catenin pathway is sufficient and necessary to effect microglia activation state.

Wnt/ β -catenin pathway activity negatively correlates with pro-inflammatory microglia activation *in vivo*

We further tested our working hypothesis that Wnt/ β -catenin signalling drives a pro-inflammatory phenotype in MG/M ϕ *in vivo* using non-cell specific approaches in zebrafish and mice and then transgenic mice with MG/M ϕ specific β -catenin knock-down. In zebrafish larvae at 72 hpf that express RFP in MG/M ϕ (Tg[pU1::Gal4-UAS-TagRFP]) we injected

Figure 2 Continued

complexity index in GFP+ MG/M ϕ at P3 (scale bar = 25 μ m). (C) MG/M ϕ phenotype over time is represented by min to max box and whiskers plots of pro-inflammatory, anti-inflammatory and immuno-regulatory markers levels by RT-qPCR in CD11B+ MG/M ϕ from brain in PBS or IL-1 β injected mice. See also Supplementary Figs 1, 2 and Supplementary Table 5. mRNA levels are presented as a fold-change relative to PBS group. Two-way ANOVA with *post hoc* Bonferroni's test, * P < 0.05, ** P < 0.01, *** P < 0.001, n /group are indicated under the legend.

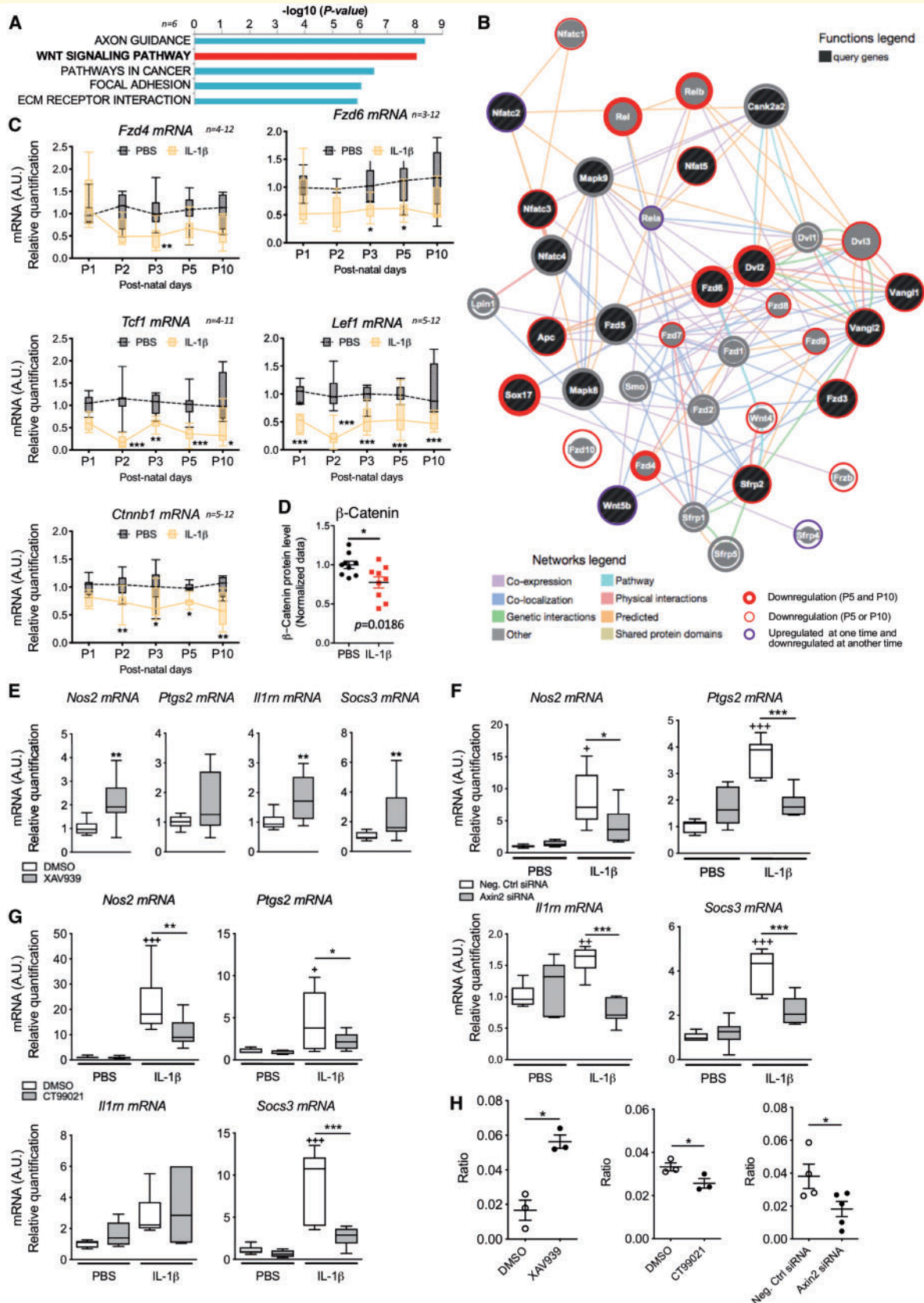


Figure 3 The Wnt pathway is downregulated in pro-inflammatory microglia and modulates microglia activation *in vitro*. (A) Transcriptomic data reveal that the Wnt signalling pathway is strongly associated with MG/Mφ activation in our model and (B) builds a cohesive network of multi-modal interactions between Wnt pathway genes in the MG/Mφ co-expression network. (C) Validation of a selection of Wnt targets from the array data showing min to max box and whiskers plots of mRNA level presented as a fold-change relative to PBS group by

(continued)

into the hindbrain the prototypical pro-inflammatory agent LPS (Fig. 4A). LPS was used because of the unavailability of recombinant zebrafish IL-1 β and prior work demonstrating the expression by zebrafish of receptors for LPS, the Toll-like 4 receptor (TLR4), and the requisite downstream signalling cascade (van der Sar *et al.*, 2006). Although LPS and IL-1 β use different signalling pathways, the end result of exposure to both is a complex neuroinflammatory milieu and it is this complex ‘soup’ and not the IL-1 β alone that is effective. We compared the nature of the IL-1 β and LPS responses in primary microglia using qRT-PCR for 12 genes to highlight the similarities in the overall inflammatory milieu induced by these inflammatory agents (Supplementary Fig. 3A), supporting our previous data comparing inflammatory protocols (Chhor *et al.*, 2013). LPS-induced neuroinflammation in the zebrafish was confirmed after 48 h by a significant increase in fluorescent MG/M ϕ in the optic tectum (Fig. 4B and C). We observe a similar increase in MG/M ϕ immunofluorescence in our mouse model with IBA1 and MAC1 immunofluorescence (Favrais *et al.*, 2011). As expected, exposure of zebrafish larvae to the Wnt/ β -catenin antagonist XAV939 exacerbated the LPS-induced MG/M ϕ activation, while conversely, exposure to Wnt agonists acting via the canonical GSK3 β dependent pathway with CT99021 or LiCl prevented the LPS-induced MG/M ϕ activation (Fig. 4B and C).

Subsequently, we studied the specific relationship between Wnt/ β -catenin pathway activity and MG/M ϕ activation in mice using pharmacological and genetic approaches. First, we inhibited the Wnt/ β -catenin pathway by intracerebroventricular injection of XAV939 in P1 pups and isolated CD11B+ MG/M ϕ 3 h later. In agreement with our hypothesis, *in vivo* Wnt inhibition with XAV939 mimicked the effects of systemic IL-1 β on gene expression in MG/M ϕ (Fig. 4D). Furthermore, to target the Wnt pathway in MG/M ϕ specifically, we bred LysM^{Cre/Cre} with β -catenin^{Flox/Flox} mice to generate β -Cat ^{Δ /+} transgenic mice. Recombination, and as such knockout of β -catenin occurs in $\geq 20\%$ of MG/M ϕ in this Cre line (Cho *et al.*, 2008; Derecki *et al.*, 2012; Degos *et al.*, 2013) and we verified that there was a 40% decrease in *Ctnnb1* mRNA encoding β -catenin ($P < 0.001$, Fig. 4E). In the absence of external inflammatory stimuli, β -Cat ^{Δ /+} mice with microglia expressing reduced

levels of β -catenin developed a myelin deficiency that mimicked the damaging effects of systemic IL-1 β exposure in our encephalopathy of prematurity model. Specifically, these mice had reduced *Mbp* mRNA in the anterior cortex at P10 (Fig. 4F) and reduced MBP immunoreactivity in the corpus callosum and cingulum at P30 (Fig. 4G and H).

Collectively, these data show that in fish and mice that downregulation of the Wnt pathway is sufficient and necessary to drive a pro-inflammatory MG/M ϕ activation state. Of note, even a partial MG/M ϕ -specific β -catenin deletion *in vivo* in the absence of any external stimuli is sufficient to induce MG/M ϕ activation leading to a myelination defect.

The Wnt pathway regulates activation state in primary human microglia *in vitro*

We then verified a similar relationship between decreased Wnt and increased pro-inflammatory activation in primary human MACSed CD11B+ MG/M ϕ isolated from cerebral tissues collected from scheduled terminations at gestational age 19 and 20 weeks. Based on the low numbers of cells available we aimed to ensure we induced a robust response so we chose to use LPS to induce a pro-inflammatory microglia response based on previous studies (Melief *et al.*, 2012). Human primary MG/M ϕ were activated to a pro-inflammatory state as indicated by modified morphology (Fig. 5A) and increased *PTGS2* (COX2) gene expression (Fig. 5B). In agreement with observations in our mouse and zebrafish experiments these pro-inflammatory activated human primary microglia had a reduction in their expression of mRNA for the β -catenin gene, *CTNNB1* (Fig. 5C).

Genomic variance in Wnt pathway genes is relevant to human preterm infant white matter structure

Our experimental data show that genetic knockdown of Wnt/ β -catenin signalling is sufficient in itself to drive brain injury in transgenic mice. In a conceptually similar manner, but with an expected much smaller effect size, we

Figure 3 Continued

RT-qPCR in CD11B+ MG/M ϕ from PBS or IL-1 β -exposed mice. See also Supplementary Fig. 3. Two-way ANOVA, *post hoc* Bonferroni's test, * $P < 0.05$, ** $P < 0.01$, *** $P < 0.001$, *n*/group is indicated on the graph. (D) Scatter plot of β -catenin protein level from ELISA in CD11B+ MG/M ϕ from PBS or IL-1 β -exposed mice at P3. Data are expressed as fold-change relative to PBS group (mean \pm SEM, Student's *t*-test, * $P < 0.05$, *n* = 9/group). (E) β -Catenin pathway inhibition, with XAV939, induced a pro-inflammatory like activation in primary microglia. Min to max box and whiskers plots of mRNA levels are presented as a fold-change relative to vehicle group (Student's *t*-test, * $P < 0.05$, ** $P < 0.01$, *n* = 12/group). (F) β -Catenin pathway activation induced by blocking *Axin2* with siRNA (see also Supplementary Fig. 3I, $\sim 45\%$ *Axin2* mRNA decrease). (G) Inhibition of GSK3 β , a β -catenin inhibitor, with CT99021 reduced primary microglia activation induced by IL-1 β . Min to max box and whiskers plots of mRNA levels presented as a fold-change relative to vehicle group. One-way ANOVA with *post hoc* Newman-Keuls's test. Effects of IL-1 β on gene expression are shown with * $P < 0.05$, ** $P < 0.01$, *** $P < 0.001$; effects of *Axin2* siRNA or CT99021 to alter the IL-1 β effects are shown with * $P < 0.05$, ** $P < 0.01$, *** $P < 0.001$, *n* = 6/group). (H) Effects of modulating Wnt with XAV939, *Axin2* siRNA and CT99021 on phosphorylation of β -catenin (PSer45 β -catenin/ β -catenin ratio) in primary microglia. Scatter plots, mean \pm SEM, Mann-Whitney test * $P < 0.05$, *n* = 3/group.

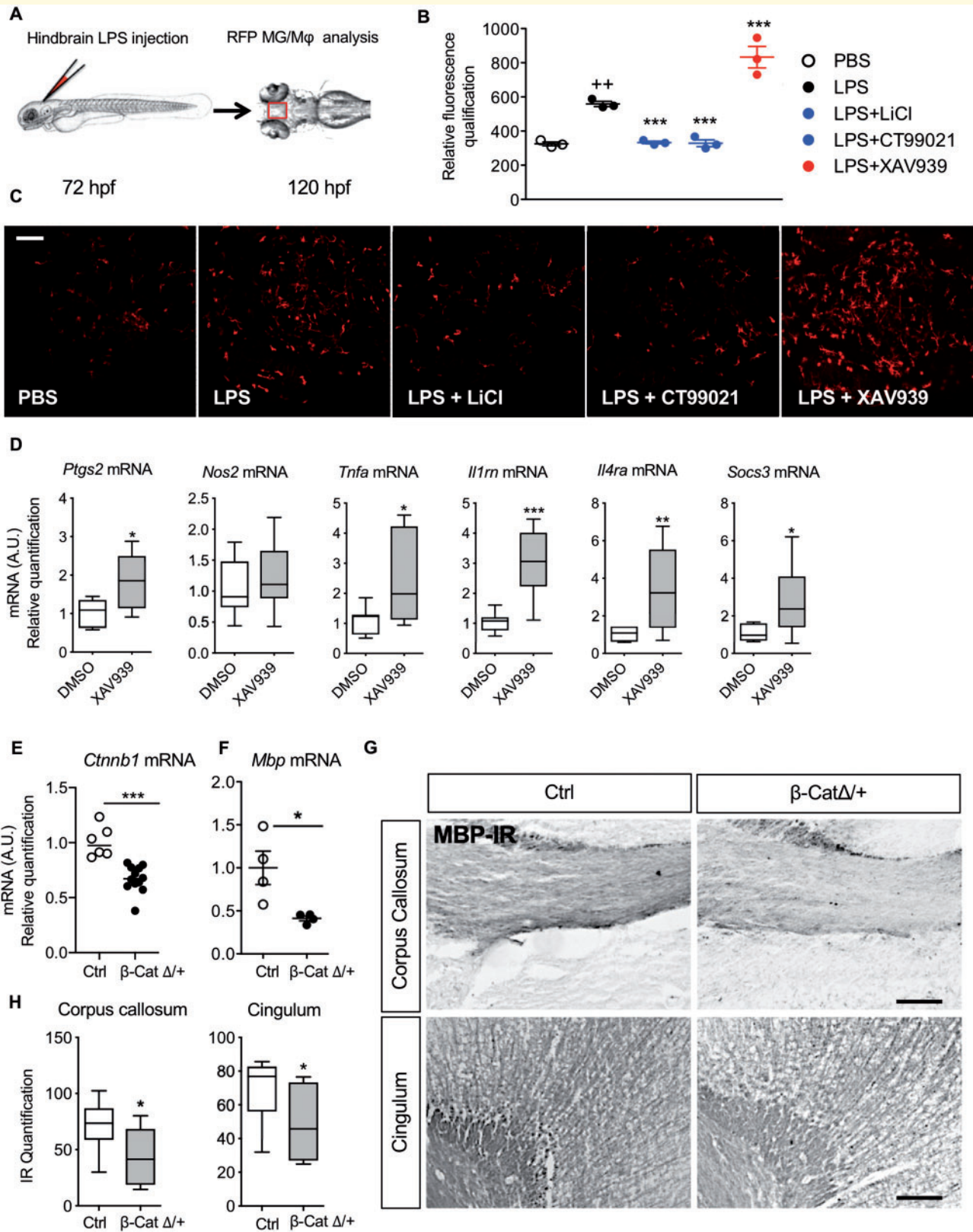


Figure 4 Wnt/ β -catenin pathway regulates MG/M ϕ activation and hypomyelination *in vivo*. Wnt signalling was modulated *in vivo* with pharmacological techniques in zebrafish (A–C) and mice (D) and using gene knockout in mice (E–G). (A) Location of LPS microinjection (5 ng/injection) into the zebrafish hindbrain at 72 hpf in *pu1::Gal4-UAS::TagRFP* morpholinos followed by analysis at 120 hpf. (B) Scatter plot of quantification of RFP labelled microglia and (C) representative images of RFP microglia in these zebrafish brains after LPS injection in the presence or not in their growth solution of Wnt/ β -catenin pathway activators LiCl (80 mM) and CT99021 (3 μ M) or Wnt inhibitor XAV939 (5 μ M) (mean \pm SEM, one-way ANOVA with *post hoc* Newman-Keuls's test, ** P < 0.01, *** P < 0.001). Scale bar = 40 μ m. (D) Analysis of the phenotype of

(continued)

reasoned that genetic variation in Wnt pathway genes would be associated with surrogates of white matter-mediated connectivity in infants born preterm. We hypothesized that, at least in part, any link between WNT variation and connectivity would be mediated by differences in the innate response to inflammatory challenge in these preterm infants. Although our genetic analysis is agnostic with respect to cellular mechanism or type, a link between WNT variations and brain structure would support further research into WNTs role in injury, and using WNT variants for preterm-born infant injury/outcome stratification. To test our prediction of a link between WNT and preterm brain connectivity we performed an analysis where we jointly analysed connectivity data derived from MRI and genomics data from 290 preterm-born infants. This approach has previously uncovered novel genetic variants associated with brain connectivity phenotype (Krishnan *et al.*, 2016, 2017). The preterm-born infants included in this study are described in more detail in Supplementary Table 4 and the inclusion/exclusion criteria are outlined in the ‘Materials and methods’ section. Imaging of the white matter in preterm-born infants associates with neurodevelopmental outcomes in preterm-born infants (Woodward *et al.*, 2006; Spittle *et al.*, 2009; Pandit *et al.*, 2013), making an imaging-genomics approach relevant for generating hypotheses about the relevance of the Wnt pathway to functional outcomes for preterm-born infants.

In this paired imaging-genomics analysis, we assessed SNPs in our preterm cohort. SNPs are DNA sequence variations where a single nucleotide varies between individual members of a species that can help pinpoint contributions of specific genes to disease states. To define the intracerebral anatomical connectivity phenotype in our preterm cohort, we used 3 T diffusion MRI and optimized probabilistic tractography as described previously (Robinson *et al.*, 2008; Shi *et al.*, 2011), adjusting the results for post-menstrual age at scan and at birth. Regions of interest for seeding tractography were obtained by segmentation of the brain based on a 90-node anatomical neonatal atlas (Shi *et al.*, 2011) focusing on cortico-cortical connections. DNA extracted from saliva was genotyped and a gene-set of-interest defined using SNPs in the WNT signalling pathway (entry hsa04310) of the KEGG database ($n = 141$ genes).

SNPs were mapped to all of the genes in the KEGG Wnt pathway using the JAG tool and Genome Reference Consortium Human Build 37 (GRCh37; hg19), using 2 kb up/downstream, in line with NCBI practices (NCBI, 2005). Following SNP-gene mapping, we tested the null hypothesis that variation in Wnt pathway genes is not associated with the preterm tractography phenotype using JAG (Lips *et al.*, 2015). Specifically, genes in the WNT-set were tested in two ways (Fig. 5D). First, we performed a ‘competitive/enrichment test’ to determine whether the Wnt pathway genes were no more associated with the connectivity phenotype than 300 randomly drawn non-WNT-pathway gene-sets. Second, we performed a ‘self-contained/association test’ to determine whether there is a comparable association between the original connectivity phenotype and WNT, versus 1000 random permutations of the phenotype and WNT. The ‘competitive test’, in which we compared to randomly generated sets of genes, showed a significant enrichment of genetic variants associated with the phenotype in the WNT gene-set compared to random gene sets (empirical $P = 0.037$, Fig. 5E inset). The conservative ‘self-contained’ test in which we compared to 1000 permuted phenotypes indicated that the WNT signalling gene-set was associated with our phenotype; i.e. white matter probabilistic tractography features (empirical $P = 0.064$; Fig. 5E histogram and inset). We performed a gene-by-gene analysis of SNPs within the WNT signalling gene-set to investigate which genes might be predominantly contributing to the collective pathway enrichment signal. This test highlighted a group of 10 genes with individual significant association with the tractography phenotype (empirical $P \leq 0.05$, 1000 permutations). These 10 genes included eight associated with Wnt/ β -catenin signalling *NFATC4*, *CSNK1A1*, *MAPK10*, *WNT2B*, *SMAD3*, *FBXW11*, *NLK*, *CSNK1A1L*, and two associated with the Wnt/ Ca^{2+} or Wnt/PCP pathways, *PLCB2* and *WNT5A* (Table 1, Fig. 5F and Supplementary Table 7). Although, we cannot determine specifically how these SNP variants would alter the brain phenotype we found using the Genome-scale Integrated Analysis of gene Networks in Tissues (GIANT) tool that these genes created a coherent interaction network within a human brain-specific gene interaction network (Fig. 5G and Supplementary Table 8). GIANT hosts searchable genome-scale functional

Figure 4 Continued

CD11B+ cells isolated from PI mice injected intracerebroventricularly with XAV939 (0.5 nmol) alone (no intraperitoneal IL-1 β), demonstrating increased MG/M ϕ activation with Wnt agonism. Min to max box and whiskers plots of quantification of *Nos2*, *Ptgs2*, *Tnfa*, *Il1rn*, *Socs3* and *Il4ra* mRNA by RT-qPCR. mRNA levels are presented as a fold-change relative to PBS/DMSO group (Student’s *t*-test, * $P < 0.05$, ** $P < 0.01$ and *** $P < 0.001$ $n = 7$ –10/group. (E and F) β -Catenin deficit in microglia driven by β -catenin^{flox/+}/LysM^{Cre/+} (β -catenin ^{Δ /+}) induces hypomyelination. Scatter plots of quantification by RT-qPCR of (E) *Ctnnb1* mRNA deficit in CD11B+ MG/M ϕ from P10 β -catenin ^{Δ /+} mice ($n = 6$ –12/group) and (F) *Mbp* mRNA deficit in the anterior brain at P10 in β -catenin ^{Δ /+} mice. mRNA levels are presented as a fold-change relative to control (Ctrl) mice (β -catenin^{+/+}/LysM^{Cre/+}) ($n = 4$ /group) (mean, Mann-Whitney test, * $P < 0.05$, *** $P < 0.01$). (H) Min to max box and whiskers plot of grey density level of MBP immunoreactivity (MBP-IR) in the corpus callosum and cingulum at P30 relative to control mice. (Mann-Whitney test, * $P < 0.05$, $n = 6$ /group and illustrated by representative images of MBP-IR in G. Scale bar = 40 μ m.

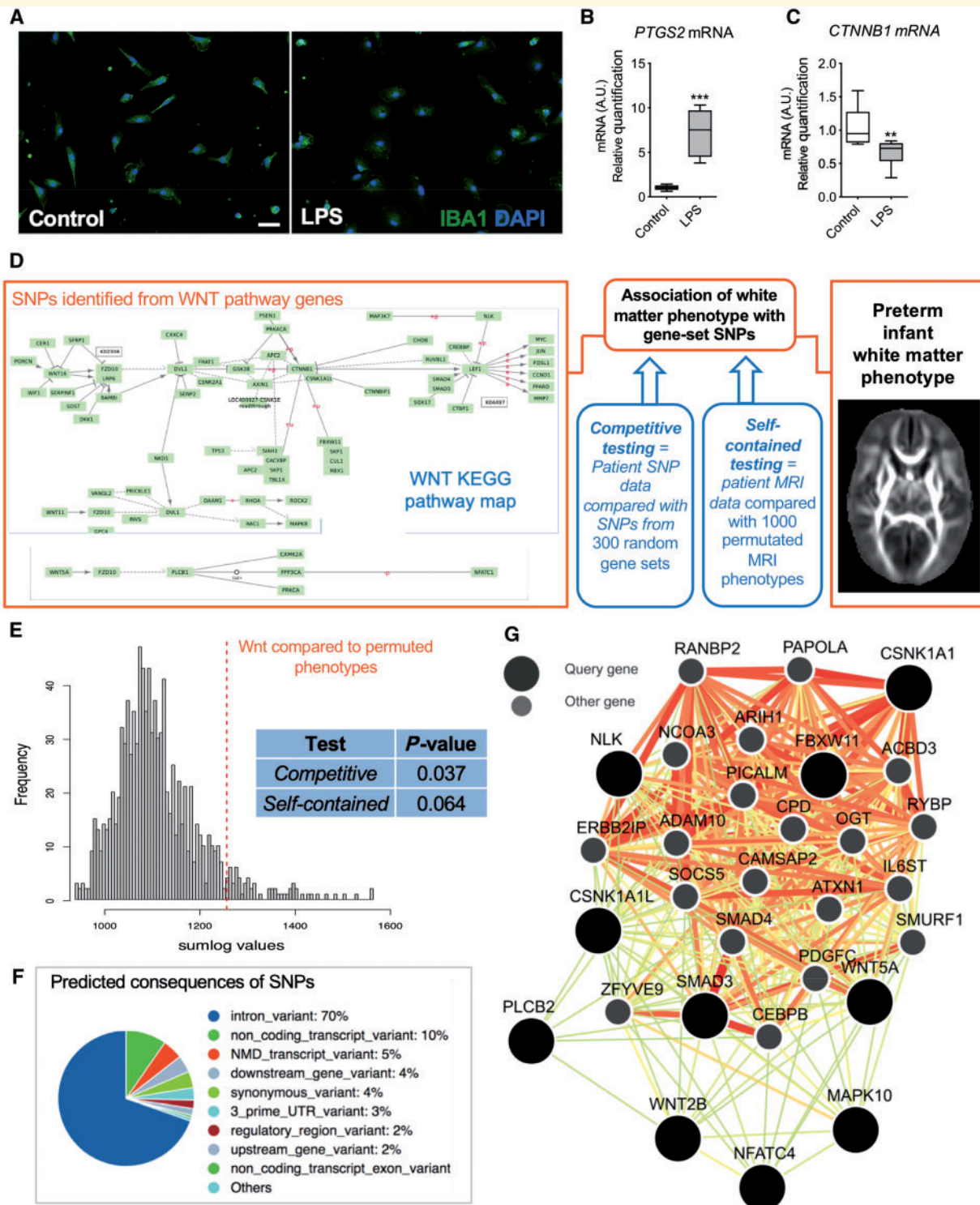


Figure 5 Human microglia activation leads to Wnt/ β -catenin downregulation and genetic variation in the Wnt pathway associates with preterm infant white matter phenotype. (A) Human primary microglia exposed to LPS showing immunoreactive changes with IBA1 (scale bar = 50 μ m); (B) upregulated mRNA expression for COX2 (*PTGS2*); and (C) the associated decrease in the expression of the gene for β -catenin (*CTNNB1*). Min to max box and whiskers plots, Student's *t*-test, ** $P < 0.01$, *** $P < 0.0001$, $n = 6-9$ /group. (D) Schematic of the analysis for any association between SNPs in the Wnt pathway and the preterm infant white matter phenotype. Common genetic variation (SNPs) in the WNT gene-set were enriched for variants associated with tractography features when compared to random matched gene-sets, i.e. competitive test, $P = 0.037$, 1000 permutations, (E, blue inset) and is also associated with white matter probabilistic tractography in preterm infants, compared with the null background, i.e. self-contained test, $P = 0.064$, 1000 permutations (E, blue inset). (F) The predicted consequences of all of the SNPs found in the top 10 ranked WNT genes shown in Table 1, a total of 42 SNPs. (G) The relationships between these 10 genes significantly associated with the tractography phenotype is reconstructed in a high confidence interaction network specific to the human brain, retrieved from known tissue-specific expression and regulatory data (Greene et al., 2015).

maps of human tissues, integrating an extensive collection of experimental datasets from publications including expression, regulatory and protein data (Greene *et al.*, 2015). We also performed an exploratory investigation of function for the 42 SNPs from the 10 genes predominantly contributing to the collective pathway enrichment signal to provide information related to function. We used the Gene Effect Predictor within the Consortium Human Build 37 (GRCh37; hg19) tool to study the 42 SNPs, whose full details are given in Supplementary Table 9. All 42 SNPs existed in the database and they were predicted to have 463 consequences on the genome (Supplementary Table 10). Specifically, these SNPs overlapped with 103 separate gene transcripts, seven of them overlapped regulatory sequences and overall 95% were synonymous variants and 5% were missense variants (Fig. 5F).

These linked imaging-genomic analyses demonstrate a relationship between genetic variation in the Wnt pathway and an important clinical phenotype. They provide adjunct support for a causal relationship between the Wnt pathway and the brain phenotype that has been established with our experimental data.

The neuroprotective effects of a Wnt pathway agonist delivered via 3DNA nanocarrier

There is a paucity of neurotherapeutic options for damage to the preterm-born infant brain and many other neuroinflammatory-mediated neurological disorders. We have clearly demonstrated a link between decreased Wnt/ β -catenin pathway activation and a pro-inflammatory microglia activation state. In addition, we have shown the relevance of this pathway in human microglia and preterm infant brain structure. As such, we complete this study by demonstrating that the Wnt pathway is a viable therapeutic target. To achieve this, we specifically increased Wnt pathway activity in MG/M ϕ using a peptide inhibitor of GSK3 β , which has the effect of preventing the formation of the β -catenin degradation complex. We delivered this peptide to MG/M ϕ *in vitro* and *in vivo* by conjugating it to a 3DNA nanocarrier together with a fluorescent tag (Cy3) (Genisphere). 3DNA nanocarriers are interconnected monomeric subunits of DNA of \sim 200 nm in diameter that are intrinsically capable of endosomal escape (Muro, 2014). In brief, we validated that our 3DNA-peptide conjugate had microglia specificity and immunomodulatory efficacy *in vitro*, that it crosses the blood–brain barrier, that it has cell specificity *in vivo*, and finally that it is neurotherapeutic *in vivo* in our systemic-inflammation (IL-1 β) driven model of encephalopathy of the preterm-born infant.

First, we demonstrated *in vitro* that 3DNA nanocarrier Cy3 tagged conjugates are specifically internalized by microglia in mixed glial cultures (Supplementary Fig. 5A) and by microglia in primary cultures after 4 h of incubation (Supplementary Fig. 5B). When 3DNA was conjugated to

both Cy3 and the peptide L803mts, an agonist of canonical Wnt signalling via inhibition of GSK3 β , it was also specifically internalized by microglia in primary culture (Supplementary Fig. 6A). We also used the 3DNA nanocarrier tagged with Cy3 to deliver a cargo of L803mts to MG/M ϕ that had been activated with IL-1 β *in vitro*. Treatment of primary microglia with L803mts delivered with 3DNA reversed the IL-1 β -induced activation of the microglia but had no effect on PBS-treated microglia as assessed with gene expression analysis (Supplementary Fig. 6B).

Moving *in vivo*, we aimed to generate the proof-of-concept that the 3DNA nanocarrier delivering L803mts and tagged with Cy3 can be taken up by MG/M ϕ and influence MG/M ϕ phenotype. Specifically, the L803mts and Cy3 conjugated 3DNA nanocarrier or the scrambled (SCR) peptide control and Cy3 conjugated 3DNA nanocarrier was injected intracerebroventricular into P1 mice, 1 h prior to our standard intraperitoneal IL-1 β injection. Four hours after intracerebroventricular injection, we observed Cy3 fluorescence exclusively co-localized with IBA-1+ staining in the periventricular white matter (Fig. 6A and Supplementary Video 1). In the same paradigm, using qRT-PCR analysis of isolated CD11B+ MG/M ϕ we demonstrated that intracerebroventricularly delivered 3DNA loaded with L803mts and tagged with Cy3 reversed the effect of IL-1 β on the MG/M ϕ phenotype but that the 3DNA-L803mts-Cy3 had no significant effect on MG/M ϕ from PBS-treated mice (Fig. 6B). As intracerebroventricular injections cause aggravated tissue injury we subsequently undertook a translationally orientated trial using intraperitoneal delivery of Cy3-tagged 3DNA conjugated to L803mts. The 3DNA L803mts Cy3 or 3DNA SCR Cy3 control was injected intraperitoneal daily between P1 and P5, in parallel with PBS or IL-1 β . At P5, immunofluorescence in the anterior periventricular white matter confirmed that 3DNA L803mts Cy3 was specifically taken up by IBA1+ MG/M ϕ (Fig. 7A). We also assessed uptake of our 3DNA conjugate by populations of macrophage in the body after intraperitoneal delivery at P5. Using the same immunohistochemistry techniques that clearly show uptake in MG/M ϕ we did not find Cy3 positive staining in the spleen or liver (Supplementary Fig. 5C and D).

To validate the *in vivo* neurotherapeutic efficacy of our novel nanocarrier-mediated WNT agonist therapy, we assessed the IL-1 β -induced myelination deficit by measuring *Mbp* mRNA at P10, MBP protein via western blotting at P15 and axonal myelination via electron microscopy at P30. We have previously shown in this model that there is an accumulation of immature oligodendrocytes (NG2+ and PDGFR α +), reduced small calibre axonal myelination and reduced expression of myelin proteins (Favrais *et al.*, 2011; Schang *et al.*, 2014; Rangon *et al.*, 2018). Treatment with intraperitoneal 3DNA L803mts Cy3 significantly prevented the IL-1 β -induced reduction in *Mbp* mRNA (Fig. 7B) and alleviated the IL-1 β -induced reduction in MBP proteins (Fig. 7C, D and Supplementary Fig. 7A).

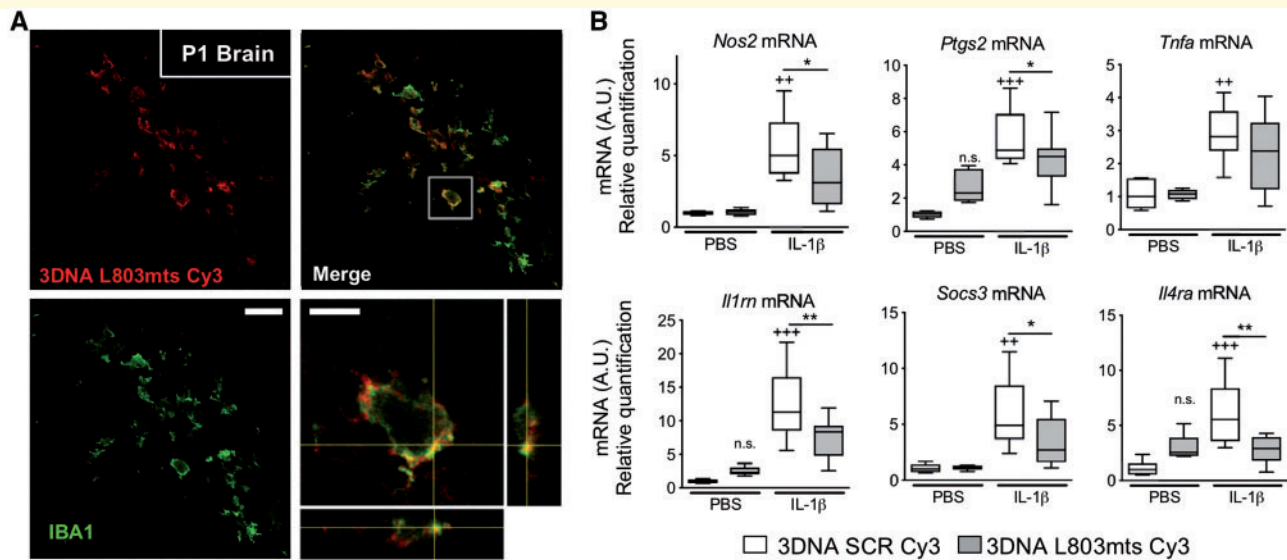


Figure 6 Nanocarrier delivery of a Wnt/ β -catenin pathway activator L803mts regulates MG/M ϕ activation in our encephalopathy of prematurity model. **(A)** Representative images of the *in vivo* uptake of 3DNA by IBA1⁺ cells in the subventricular white matter 4 h after intracerebroventricular administration of 3DNA SCR Cy3 (control) or 3DNA L803mts Cy3 (200 ng); scale bar = 40 μ m. *Bottom right* panel shows orthogonal view of white box inset showing co-localization in detail, scale bar = 10 μ m. See also Supplementary Figs 4A, B, 5, and Supplementary Video 1. **(B)** Min to max box and whiskers plots of *Nos2*, *Ptgs2*, *Tnfa*, *Il1m*, *Socs3* and *Il4ra* mRNA by qRT-PCR in CD11B⁺ MG/M ϕ cells from intracerebroventricular injected PBS or IL-1 β -treated mice with 3DNA SCR Cy3 or 3DNA L803mts at P1. mRNA levels are presented as a fold-change relative to vehicle group (one-way ANOVA with *post hoc* Newman-Keuls's test, $^{*}P < 0.01$, $^{***}P < 0.001$ for statistically significant difference between the PBS and IL-1 β groups also exposed to 3DNA SCR Cy3. $^{*}P < 0.05$, $^{**}P < 0.01$ for the effects of 3DNA Wnt modulator delivery, $n = 5$ –6 for PBS groups and $n = 9$ for IL-1 β groups).

Finally, we observed that these effects of 3DNA L803mt Cy3 to improve *MBP* mRNA and *MBP* protein levels correlated with improvements in axonal myelination, as indicated by the decrease of G-ratio of fibres of 0.2 to 0.8 μ m diameter in the corpus collosum (Fig. 7E and F).

To evaluate whether this improvement in neuropathology with nanocarrier-mediated treatment also reverses the behavioural deficits observed in adults in this paradigm, spatial learning and memory were assessed starting at P90. First we tested basic behavioural parameters by spontaneous locomotion and rearing using actimetry, and exploratory behaviour using an open field test. This injury model is designed to induce subtle neurobehavioural deficits to mimic the learning problems that become apparent in school age children born preterm (Lindstrom *et al.*, 2011; Spittle *et al.*, 2017). As expected, no changes in these basic parameters was observed between groups of mice, i.e. controls (PBS + 3DNA SCR Cy3), injured (IL-1 β + SRC Cy3) or the treatment group (IL-1 β + 3DNA L803mts Cy3) (Supplementary Fig. 7B and C). Spatial learning and memory were tested via the Barnes maze test, which assesses spatial learning over 5 days of probe trials plus short term memory retention at the end of the learning trials and long term memory retention 10 days later. Spatial learning (i.e. distance travelled and number of errors) itself was not modified by IL-1 β exposure (Fig. 7G). However, mice exposed to IL-1 β had a short-term memory deficit based on a decreased distance travelled

in the target sextant during the first 30 s of the probe trial on the final day of testing (Fig. 7H). In addition, IL-1 β exposure caused deficits in long term memory recall, as assessed as the increased distance travelled in a single probe trial at 10 days post-learning (Fig. 7I). These short term and long term neuroinflammatory induced memory deficits were both reversed by intraperitoneal treatment by delivery to MG/M ϕ of the Wnt antagonist, L803mts (3DNA L803mts Cy3) by the 3DNA nanocarrier (Fig. 6H and I).

Altogether these data clearly demonstrate that a Wnt agonist therapy can reduce pro-inflammatory MG/M ϕ activation and improve neuropathological and functional outcomes in a model of neuroinflammation mediated white matter injury. These data also highlight a novel 3DNA nanocarrier that has the ability to deliver therapies like this *in vivo* specifically to microglia.

Discussion

Recent research has highlighted that microglia of the developing brain have a unique phenotype. The aims of this study were to identify in microglia of the developing brain the molecular regulators of injury-related phenotype, and to validate them as therapeutic targets for preventing microglia-mediated injury in the 15 million infants born preterm every year. We undertook a comprehensive set of

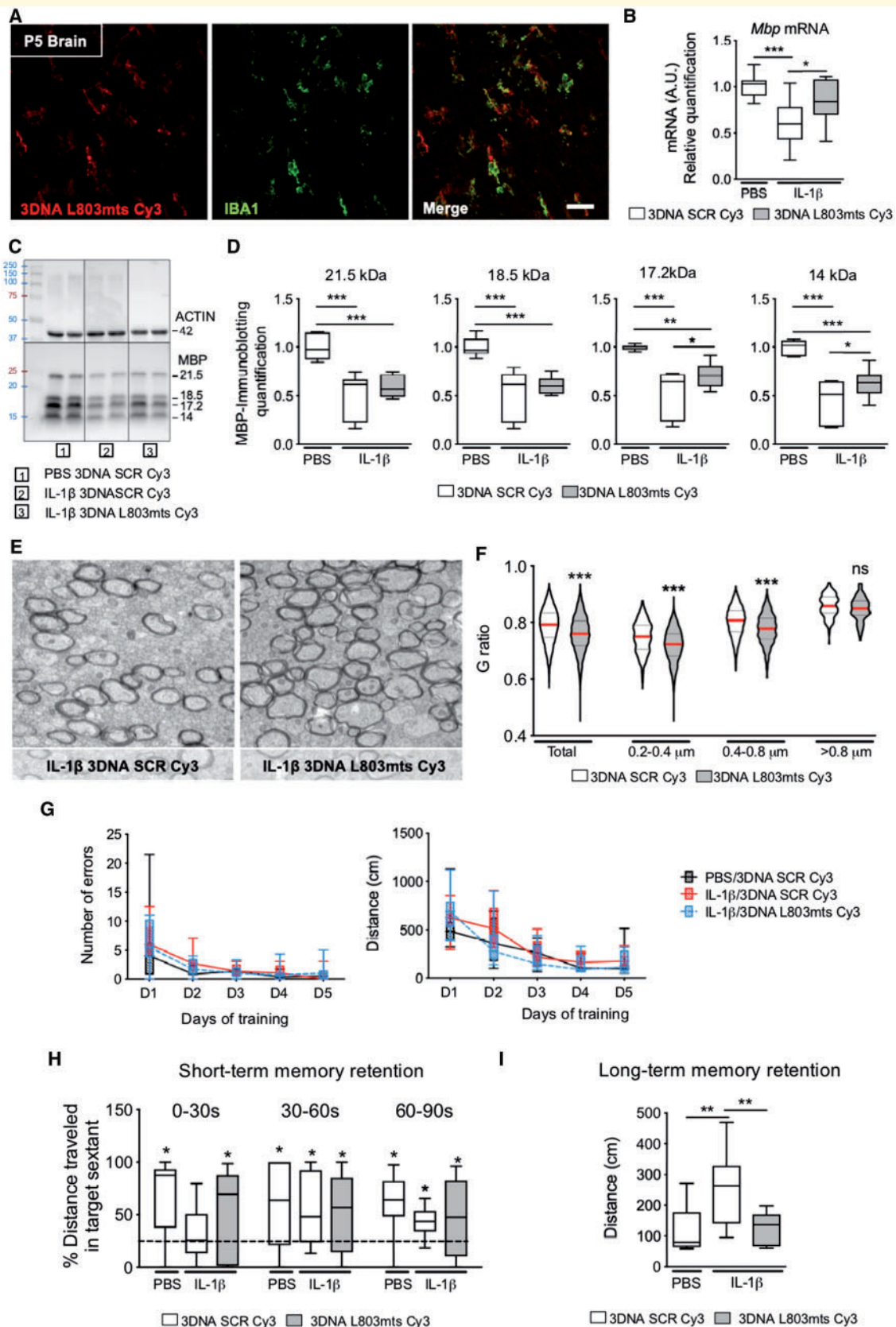


Figure 7 Nanocarrier delivery of a Wnt/ β -catenin pathway activator L803mts in microglia reduces IL-1 β -induced hypomyelination and memory deficit. **(A)** Representative images of *in vivo* uptake of 3DNA by IBA1⁺ cells in subventricular white matter at P5 after intraperitoneal injections of 3DNA L803mts Cy3 or 3DNA SCR Cy3 (500 ng/injection). Scale bar = 40 μ m. **(B)** Min to max box and whiskers plot of *Mbp* mRNA by qRT-PCR in the anterior brain of mice at P10. mRNA levels are presented as a fold-change relative to the 3DNA SCR Cy3/PBS

Table 1 Functional descriptions of the 10 genes within the WNT gene-set

Gene symbol	Description	Adjusted P-value	nSNP
NFATC4	Nuclear factor of activated T-cells, cytoplasmic, calcineurin-dependent 4	0.001	9
CSNK1A1	Casein kinase I, alpha 1	0.002	52
MAPK10	Mitogen-activated protein kinase 10	0.002	4
WNT2B	Wingless-type MMTV integration site family, member 2B	0.007	6
SMAD3	SMAD family member 3	0.014	57
FBXW11	F-box and WD repeat domain containing 11	0.015	4
WNT5A	Wingless-type MMTV integration site family, member 5A	0.023	12
NLK	Nemo-like kinase	0.026	11
CSNK1A1L	Casein kinase I, alpha 1-like	0.033	11
PLCB2	Phospholipase C, beta 2	0.038	5

Table shows SNPs that were most significantly associated with the preterm infant tractography phenotype outlined in Fig. 5D and E. The predicted consequences of changes in these genes is found in Fig. 5F.

nSNP = number of SNPs in the gene.

studies involving pharmacological and genetic manipulations in mouse and zebrafish models, human tissue and patient data. We also introduced an innovative 3DNA nanocarrier that can deliver drugs specifically to microglia *in vivo*. Initially, we characterized the complex MG/M ϕ phenotype in our mouse model of encephalopathy of prematurity (Favrais *et al.*, 2011; Schang *et al.*, 2014; Krishnan *et al.*, 2017) and demonstrated that MG/M ϕ activation is directly responsible in this model for the clinically relevant myelination defect. Next, using a genome-wide transcriptomic analysis of these activated MG/M ϕ we associated the Wnt pathway with MG/M ϕ activation. We specifically determined that the expression of Wnt/ β -catenin pathway receptors, ligands and intracellular signalling components were robustly downregulated in MG/M ϕ isolated from our animal model. A combination of approaches in zebrafish and mouse models *in vitro* and *in vivo* allowed us to determine that Wnt/ β -catenin pathway inhibition specific to MG/M ϕ is sufficient and necessary to induce in these cells a pro-inflammatory activation, and subsequent hypomyelination *in vivo*. We highlighted the relevance of the Wnt pathway to the activation state of human primary microglia, and preterm-born infant brain development. Of note, we verified our prediction that genetic variation in the

Wnt pathway in preterm infants is related to indices of their cerebral structural connectivity. Although, it is a limitation of these types of human studies that the data are not cell specific and the effects of the WNT SNPs may be on earlier stages of development in other cell types. Finally, we selectively delivered to MG/M ϕ *in vivo* a Wnt pathway activator using a 3DNA nanocarrier, which we administered via non-invasive intraperitoneal injection. This specific and non-invasive delivery of a Wnt agonist therapeutic prevented a pro-inflammatory MG/M ϕ activation state and the associated white matter damage and cognitive deficit in our mouse model. Together, these data demonstrate that downregulation of the canonical Wnt/ β -catenin pathway triggers a hypomyelination-inducing microglia phenotype and validate this pathway as a novel and clinically viable neurotherapeutic target thanks to the MG/M ϕ specificity of 3DNA nanocarriers.

Our evidence supports that the Wnt pathway controlling MG/M ϕ phenotype is the canonical Wnt/ β -catenin pathway. Our supporting data include that genetic and pharmacological manipulation of the β -catenin degradation complex via AXIN2 robustly effected MG/M ϕ phenotype *in vitro* and *in vivo*. In contrast, blockade of non-canonical Wnt signalling with a PKC inhibitor had no effect on

Figure 7 Continued

group (one way-ANOVA with Newman-Keuls's test, * $P < 0.05$, ** $P < 0.01$, $n = 9$ –12/group). See also Supplementary Fig. 5C and D. (C) Representative image of actin and MBP immuno-blot; and (D) the min to max box and whiskers plots of quantification of the four isoforms of MBP in the anterior brain of mice at P15. Protein levels were normalized to actin and are presented as a fold-change relative to the 3DNA SCR Cy3/PBS group (one way-ANOVA with Newman-Keuls's test, * $P < 0.05$, ** $P < 0.01$, *** $P < 0.001$, $n = 6$ –8/group). (E) Representative image of electron microscope (EM) image of the corpus callosum from mice at P30. (F) Violin plots of the G-ratios from the EM analysis showing improvements in the Wnt agonist group, 3DNA L803mts (Kruskall-Wallis test, *** $P < 0.001$, $n = 4$ –5/group). Microglial targeted Wnt agonism also induced functional improvements. (G) Data from trials of the Barnes maze for spatial learning. (H) Short-term memory retention and (I) long-term memory retention in 3-month-old mice. See also Supplementary Fig. 6. Memory retention present in the 30-s trial period on Day 5 of the test (probe trial, in H) was measured by recording of the distance travelled in the target sextant (min to max box and whiskers plot, univariate t -test * $P < 0.05$, $n = 10$ /group). (I) The long-term memory deficits were measured via the distance travelled to reach the target on the 15th day after the start of testing (min to max box and whiskers plot, one-way ANOVA with Bonferroni *post hoc* was used ** $P < 0.01$, $n = 9$ /group).

microglia activation. Although, we acknowledge that there may still be a role for other facets of non-canonical signaling in the complexity of MG/M ϕ functions. However, MG/M ϕ -specific β -catenin ablation *in vivo* in-of-itself was sufficient to recapitulate the systemic-inflammation-driven hypomyelination that we see in our animal model of encephalopathy of prematurity. We also found that the WNT genes with variance associated with preterm infant connectivity were predominantly (8/10) from the Wnt/ β -catenin pathway. A key role for β -catenin would also begin to explain our observations of Wnt-mediated pro-inflammatory activation via TLR-4 and IL-1 receptor agonists and also conversely Wnt-mediated anti-inflammatory activation via a IL-4 receptor agonist. Downstream signalling of both the TLR/IL-1 and IL-4 receptor families includes activation of the transcription factor NF- κ B (nuclear factor kappa-light-chain-enhancer of activated B cells) (Caamano and Hunter, 2002). The ability of NF- κ B to mediate the opposing effects of these receptors on microglia phenotype is conferred by interactions with other regulatory factors, including at multiple levels indirectly and directly by β -catenin (Ma and Hottiger, 2016).

Ours is the first study to demonstrate a robust cell-intrinsic role of the Wnt/ β -catenin pathway in microglia activation *in vitro* and *in vivo* and validate that this pathway is a viable immunomodulatory neurotherapeutic. Previous work on Wnt and microglia has been limited to *in vitro* ligand-receptor interactions, specifically WNT3A or WNT5A. However, the specific Wnt pathway activated by a Wnt ligand is dependent on the context of ligand-receptor interaction and not only cell-intrinsic properties (van Amerongen *et al.*, 2008). This fact likely explains the discordance between the data from the previous studies, where in some paradigms Wnt exposure is anti-inflammatory (Halleskog *et al.*, 2012; Yu *et al.*, 2014) or in others the exposure was pro-inflammatory (Halleskog *et al.*, 2011; Hooper *et al.*, 2012; Halleskog and Schulte, 2013) with no relation to the predicted canonical or non-canonical pathway being activated. Altogether these data highlight the difficulty that would be faced in using ligand-receptor interactions to target the Wnt pathway to modulate microglia activity, in contrast with our success of targeting the intracellular cascade of Wnt/ β -catenin pathway specifically using our 3DNA-mediated delivery system. We also wish to note that the Wnt pathway has well characterized roles in oligodendrocyte maturation (Fancy *et al.*, 2011; Feigenson *et al.*, 2011; Guo *et al.*, 2015; Zhao *et al.*, 2016), astrocyte activation (Cao *et al.*, 2012) and endothelial cell function (Lengfeld *et al.*, 2017). Our study builds on this understanding of the role of Wnt as a complex cell specific temporally and spatially regulated controller of brain development and response to injury.

The 3DNA nanocarrier is a powerful translational tool as is it can take agents across the blood–brain barrier following intraperitoneal injection, is specifically internalized by MG/M ϕ in the brain and it has no toxicity *in vitro* or *in vivo* in our study, or in human retinal tissue *in vitro* (Gerhart *et al.*, 2017) and in preclinical *in vivo* targeted

delivery of a ovarian cancer therapy (Huang *et al.*, 2016). Wnt activation in OPCs has previously been suggested to block their maturation by a member of our current research team (Fancy *et al.*, 2011). As such it was important that 3DNA nanocarriers allowed us to target this pathway exclusively in MG/M ϕ . 3DNA has a non-injury dependent mechanism of traversing the blood–brain barrier, as it crossed in naïve and inflammation-exposed mice, although the specific mechanism is unknown. We have previously reported that the blood–brain barrier in our mouse model of encephalopathy of prematurity is primarily intact (Krishnan *et al.*, 2017). The chemical and physical attributes of 3DNA likely precludes it from entering the brain via paracellular aqueous routes or transcellular lipophilic pathways. However, investigations of receptor-mediated transcytosis are underway, as similar aptamer-based DNA duplexes can interact with receptors such as nucleolin or transferrin (Reyes-Reyes *et al.*, 2010).

In preterm infants, it is exposure to inflammatory events that are both difficult to identify or prevent, such as chorioamnionitis and sepsis, which is the leading risk factor for white matter damage. This damage is caused by microglia-mediated neuroinflammatory processes; a link that is supported by post-mortem human studies showing microgliosis in the developing white matter of preterm-born infants (Verney *et al.*, 2010, 2012; Supramaniam *et al.*, 2013) and verified by numerous experimental paradigms (see references in Hagberg *et al.*, 2015). White matter damage in these infants is observed as diffuse white matter signal changes and reduced structural connectivity using MRI analyses (Shah *et al.*, 2008; Spittle *et al.*, 2009). In a large animal model of preterm-born infant brain injury a direct link between diffuse white matter injury and white matter gliosis has been made (Riddle *et al.*, 2011). This reduced structural connectivity in preterm-born infants is in turn strongly associated with poor neurodevelopmental outcomes (Woodward *et al.*, 2006; Ball *et al.*, 2015). As such, the purpose of our imaging-genomics analysis was to link the preclinical observations of microglial-mediated compromise of structural connectivity due to white matter injury to genetic variance that could alter the microglial inflammatory response in our preterm cohort and would affect changes in structural connectivity. Our integrated analysis of imaging and genomics demonstrated that common genetic variation in Wnt pathway genes does indeed influence brain structural connectivity features within our preterm-born infants. We fully acknowledge that the data we derived are not cell-specific and could be due to effects on the white and grey matter. However, it supports in contemporaneous infants the relevance of the Wnt pathway using an imaging modality that is currently used to assess injury and predict outcome. Also, we wish to highlight that changes to the grey matter are also evident in preterm-born infants, including changes in cortical microstructure (Ball *et al.*, 2013), interneuron distribution (Stolp *et al.*, 2019) and degeneration of axons (Back and Miller, 2014). However, the contribution of axonal injury to diffuse white matter is controversial, although it is evident in

necrotic foci that are approximated to occur in only 5% of white matter injury cases (Riddle *et al.*, 2011; Buser *et al.*, 2012). Preterm-born infants with apparent focal necrosis were excluded from our imaging-genomics analysis removing a significant contribution of a frank axonopathy from effecting the connectivity phenotype in this cohort. We cannot exclude, however, that effects on the grey matter in these infants are not important determiners of outcome and effected by changes in SNPs in genes of the Wnt pathway. In addition, we found that the Wnt pathway genes containing SNPs associated with white matter tractography phenotype belonged to a human brain-specific gene interaction network. This network further builds a case for a functional effect of WNT SNPs in human preterm infants, with consequences for the development of white matter structure (Greene *et al.*, 2015). Specific prediction of the consequences of our identified SNPs found the majority were intron variants. Previous studies in experimental animals have shown that immune cell intron variants often effect cell function by altering enhancer binding (Farh *et al.*, 2015). Altogether our clinical data build a case that these Wnt pathway SNPs may be a useful way to stratify infants who are at highest risk for white matter damage, and to improve on our currently limited prognostic abilities related to long term outcome.

In conclusion, the activity of the Wnt/ β -catenin pathway regulates MG/M ϕ activation, the Wnt pathway is relevant in human brain development, and specific agonism of the Wnt/ β -catenin pathway in MG/M ϕ *in vivo* using 3DNA nanocarrier-mediated drug delivery has a beneficial effect on MG/M ϕ phenotype, myelination and cognitive deficits. This is strong evidence that Wnt signalling modulation may be a promising therapeutic approach in encephalopathy of prematurity and, potentially, in other disorders involving MG/M ϕ -mediated neuroinflammation.

Acknowledgements

Our thanks to the children and families who participated in the study, and the nurses, doctors and scientists who supported the project. We also wish to thank Dr Dominique Langui (Institut du Cerveau et de la Moelle épinière, Hôpital Pitié-Salpêtrière, Paris, France) for providing us with access to electron microscopy facilities and Dr Manuela Zinni INSERM U1141 NeuroDiderot for access to additional molecular biology facilities.

Funding

This study was supported by grants from Inserm, Université Paris Diderot, Université Sorbonne-Paris-Cité, Investissement d'Avenir (ANR-11-INBS-0011, NeurATRIS), ERA-NET Neuron (Micromet), DHU PROTECT, Association Robert Debré, PremUP, Fondation de France, Fondation pour la Recherche sur le Cerveau, Fondation des Gueules Cassées, Roger de Spoelberch Foundation, Grace de Monaco

Foundation, Leducq Foundation, Action Medical Research, Cerebral Palsy Alliance Research Foundation Australia, Wellcome Trust (WSCR P32674) and The Swedish Research Council (2015-02493). We wish to acknowledge the support of the Department of Perinatal Imaging and Health, King's College London. In addition, the authors acknowledge financial support from the National Institute for Health Research (NIHR) Biomedical Research Centre based at Guy's and St Thomas' NHS Foundation Trust and King's College London. The views expressed are those of the author(s) and not necessarily those of the NHS, the NIHR or the Department of Health.

Competing interests

The authors report no competing interests.

Supplementary material

Supplementary material is available at *Brain* online.

References

- Back SA, Luo NL, Mallinson RA, O'Malley JP, Wallen LD, Frei B, et al. Selective vulnerability of preterm white matter to oxidative damage defined by F2-isoprostanes. *Ann Neurol* 2005; 58: 108–20.
- Back SA, Miller SP. Brain injury in premature neonates: A primary cerebral dysmaturation disorder? *Ann Neurol* 2014; 75: 469–86.
- Ball G, Counsell SJ, Anjari M, Merchant N, Arichi T, Doria V, et al. An optimised tract-based spatial statistics protocol for neonates: applications to prematurity and chronic lung disease. *Neuroimage* 2010; 53: 94–102.
- Ball G, Pazderova L, Chew A, Tusor N, Merchant N, Arichi T, et al. Thalamocortical Connectivity Predicts Cognition in Children Born Preterm. *Cereb Cortex* 2015; 25: 4310–8.
- Ball G, Srinivasan L, Aljabar P, Counsell SJ, Durighel G, Hajnal JV, et al. Development of cortical microstructure in the preterm human brain. *Proc Natl Acad Sci USA* 2013; 110: 9541–6.
- Bennett ML, Bennett FC, Liddel SA, Ajami B, Zamanian JL, Fernhoff NB, et al. New tools for studying microglia in the mouse and human CNS. *Proc Natl Acad Sci USA* 2016; 113: E1738–46.
- Billiards SS, Haynes RL, Folkert RD, Borenstein NS, Trachtenberg FL, Rowitch DH, et al. Myelin abnormalities without oligodendrocyte loss in periventricular leukomalacia. *Brain Pathol* 2008; 18: 153–63.
- Boardman JP, Walley A, Ball G, Takousis P, Krishnan ML, Hughes-Carre L, et al. Common genetic variants and risk of brain injury after preterm birth. *Pediatrics* 2014; 133: e1655–63.
- Buchanan FG, DuBois RN. Connecting COX-2 and Wnt in cancer. *Cancer Cell* 2006; 9: 6–8.
- Buser JR, Maire J, Riddle A, Gong X, Nguyen T, Nelson K, et al. Arrested preoligodendrocyte maturation contributes to myelination failure in premature infants. *Ann Neurol* 2012; 71: 93–109.
- Butovsky O, Jedrychowski MP, Moore CS, Cialic R, Lanser AJ, Gabriely G, et al. Identification of a unique TGF-beta-dependent molecular and functional signature in microglia. *Nat Neurosci* 2014; 17: 131–43.
- Caamano J, Hunter CA. NF-kappaB family of transcription factors: central regulators of innate and adaptive immune functions. *Clin Microbiol Rev* 2002; 15: 414–29.

- Cao F, Yin A, Wen G, Sheikh AM, Tauqeer Z, Malik M, et al. Alteration of astrocytes and Wnt/beta-catenin signaling in the frontal cortex of autistic subjects. *J Neuroinflamm* 2012; 9: 223.
- Chhor V, Le Charpentier T, Lebon S, Ore MV, Celador IL, Josseland J, et al. Characterization of phenotype markers and neuronotoxic potential of polarised primary microglia in vitro. *Brain Behav Immun* 2013; 32: 70–85.
- Chhor V, Moretti R, Le Charpentier T, Sigaut S, Lebon S, Schwendimann L, et al. Role of microglia in a mouse model of paediatric traumatic brain injury. *Brain Behav Immun* 2017; 63: 197–209.
- Cho IH, Hong J, Suh EC, Kim JH, Lee H, Lee JE, et al. Role of microglial IKKbeta in kainic acid-induced hippocampal neuronal cell death. *Brain* 2008; 131 (Pt 11): 3019–33.
- Dammann O, Leviton A. Inflammatory brain damage in preterm newborns—dry numbers, wet lab, and causal inferences. *Early Hum Dev* 2004; 79: 1–15.
- Degos V, Peineau S, Nijboer C, Kaindl AM, Sigaut S, Favrais G, et al. G protein-coupled receptor kinase 2 and group I metabotropic glutamate receptors mediate inflammation-induced sensitization to excitotoxic neurodegeneration. *Ann Neurol* 2013; 73: 667–78.
- Delobel-Ayoub M, Arnaud C, White-Koning M, Casper C, Pierrat V, Garel M, et al. Behavioral problems and cognitive performance at 5 years of age after very preterm birth: the EPIPAGE Study. *Pediatrics* 2009; 123: 1485–92.
- Derecki NC, Cronk JC, Lu Z, Xu E, Abbott SB, Guyenet PG, et al. Wild-type microglia arrest pathology in a mouse model of Rett syndrome. *Nature* 2012; 484: 105–9.
- Du C, Wang P, Yu Y, Chen F, Liu J, Li Y. Gadolinium chloride improves the course of TNBS and DSS-induced colitis through protecting against colonic mucosal inflammation. *Sci Rep* 2014; 4: 6096.
- Durinck S, Spellman PT, Birney E, Huber W. Mapping identifiers for the integration of genomic datasets with the R/Bioconductor package biomaRt. *Nature protocols* 2009; 4: 1184–91.
- Fancy SP, Baranzini SE, Zhao C, Yuk DI, Irvine KA, Kaing S, et al. Dysregulation of the Wnt pathway inhibits timely myelination and remyelination in the mammalian CNS. *Genes Dev* 2009; 23: 1571–85.
- Fancy SP, Harrington EP, Baranzini SE, Silbereis JC, Shioh LR, Yuen TJ, et al. Parallel states of pathological Wnt signaling in neonatal brain injury and colon cancer. *Nat Neurosci* 2014; 17: 506–12.
- Fancy SP, Harrington EP, Yuen TJ, Silbereis JC, Zhao C, Baranzini SE, et al. Axin2 as regulatory and therapeutic target in newborn brain injury and remyelination. *Nat Neurosci* 2011; 14: 1009–16.
- Farh KK, Marson A, Zhu J, Kleinewietfeld M, Housley WJ, Beik S, et al. Genetic and epigenetic fine mapping of causal autoimmune disease variants. *Nature* 2015; 518: 337–43.
- Favrais G, van de Looij Y, Fleiss B, Ramanantsoa N, Bonnin P, Stoltenburg-Didinger G, et al. Systemic inflammation disrupts the developmental program of white matter. *Ann Neurol* 2011; 70: 550–65.
- Feigenson K, Reid M, See J, Crenshaw EB, 3rd, Grinspan JB. Wnt signaling is sufficient to perturb oligodendrocyte maturation. *Mol Cell Neurosci* 2009; 42: 255–65.
- Feigenson K, Reid M, See J, Crenshaw IE, Grinspan JB. Canonical Wnt signalling requires the BMP pathway to inhibit oligodendrocyte maturation. *ASN Neuro* 2011; 3: e00061.
- Fulci G, Dmitrieva N, Gianni D, Fontana EJ, Pan X, Lu Y, et al. Depletion of peripheral macrophages and brain microglia increases brain tumor titers of oncolytic viruses. *Cancer Res* 2007; 67: 9398–406.
- Gentleman RC, Carey VJ, Bates DM, Bolstad B, Dettling M, Dudoit S, et al. Bioconductor: open software development for computational biology and bioinformatics. *Genome Biol* 2004; 5: R80.
- Gerhart J, Greenbaum M, Casta L, Clemente A, Mathers K, Getts R, et al. Antibody-Conjugated, DNA-Based Nanocarriers Intercalated with Doxorubicin Eliminate Myofibroblasts in Explants of Human Lens Tissue. *J Pharmacol Exp Ther* 2017; 361: 60–7.
- Greene CS, Krishnan A, Wong AK, Ricciotti E, Zelaya RA, Himmelstein DS, et al. Understanding multicellular function and disease with human tissue-specific networks. *Nat Genet* 2015; 47: 569–76.
- Guo F, Lang J, Sohn J, Hammond E, Chang M, Pleasure D. Canonical Wnt signaling in the oligodendroglial lineage—puzzles remain. *Glia* 2015; 63: 1671–93.
- Hagberg H, Gressens P, Mallard C. Inflammation during fetal and neonatal life: implications for neurologic and neuropsychiatric disease in children and adults. *Ann Neurol* 2012; 71: 444–57.
- Hagberg H, Mallard C. Effect of inflammation on central nervous system development and vulnerability. *Curr Opin Neurol* 2005; 18: 117–23.
- Hagberg H, Mallard C, Ferriero DM, Vannucci SJ, Levison SW, Vexler ZS, et al. The role of inflammation in perinatal brain injury. *Nat Rev Neurol* 2015; 11: 192–208.
- Halleskog C, Dijksterhuis JP, Kilander MB, Becerril-Ortega J, Villaescusa JC, Lindgren E, et al. Heterotrimeric G protein-dependent WNT-5A signaling to ERK1/2 mediates distinct aspects of microglia proinflammatory transformation. *J Neuroinflamm* 2012; 9: 111.
- Halleskog C, Mulder J, Dahlstrom J, Mackie K, Hortobagyi T, Tanila H, et al. WNT signaling in activated microglia is proinflammatory. *Glia* 2011; 59: 119–31.
- Halleskog C, Schulte G. WNT-3A and WNT-5A counteract lipopolysaccharide-induced pro-inflammatory changes in mouse primary microglia. *J Neurochem* 2013; 125: 803–8.
- Hamrick SE, Miller SP, Leonard C, Glidden DV, Goldstein R, Ramaswamy V, et al. Trends in severe brain injury and neurodevelopmental outcome in premature newborn infants: the role of cystic periventricular leukomalacia. *J Pediatr* 2004; 145: 593–9.
- Haynes RL, Billiards SS, Borenstein NS, Volpe JJ, Kinney HC. Diffuse axonal injury in Periventricular Leukomalacia as determined by apoptotic marker fractin. *Pediatr Res* 2008; 63: 656–61.
- Hickman S, Izzy S, Sen P, Morsett L, El Khoury J. Microglia in neurodegeneration. *Nat Neurosci* 2018; 21: 1359–69.
- Hillier SL, Witkin SS, Krohn MA, Watts DH, Kiviat NB, Eschenbach DA. The relationship of amniotic fluid cytokines and preterm delivery, amniotic fluid infection, histologic chorioamnionitis, and chorioamnion infection. *Obstet Gynecol* 1993; 81: 941–8.
- Hooper C, Sainz-Fuertes R, Lynham S, Hye A, Killick R, Warley A, et al. Wnt3a induces exosome secretion from primary cultured rat microglia. *BMC Neurosci* 2012; 13: 144.
- Huang YH, Peng W, Furuuchi N, Gerhart J, Rhodes K, Mukherjee N, et al. Delivery of therapeutics targeting the mRNA-binding protein HuR using 3DNA nanocarriers suppresses ovarian tumor growth. *Cancer Res* 2016; 76: 1549–59.
- Johnston MV, Hagberg H. Sex and the pathogenesis of cerebral palsy. *Dev Med Child Neurol* 2007; 49: 74–8.
- Kaidanovich-Beilin O, Eldar-Finkelman H. Long-term treatment with novel glycogen synthase kinase-3 inhibitor improves glucose homeostasis in ob/ob mice: molecular characterization in liver and muscle. *J Pharmacol Exp Ther* 2006; 316: 17–24.
- Keats EC, Dominguez JM, 2nd, Grant MB, Khan ZA. Switch from canonical to noncanonical Wnt signaling mediates high glucose-induced adipogenesis. *Stem cells (Dayton, Ohio)* 2014; 32: 1649–60.
- Krasemann S, Madore C, Cialic R, Baufeld C, Calcagno N, El Fatimy R, et al. The TREM2-APOE pathway drives the transcriptional phenotype of dysfunctional microglia in neurodegenerative diseases. *Immunity* 2017; 47: 566–81.e9.
- Krishnan ML, Van Steenwinckel J, Schang AL, Yan J, Arnadottir J, Le Charpentier T, et al. Integrative genomics of microglia implicates DLG4 (PSD95) in the white matter development of preterm infants. *Nat Commun* 2017; 8: 428.
- Krishnan ML, Wang Z, Silver M, Boardman JP, Ball G, Counsell SJ, et al. Possible relationship between common genetic variation and

- white matter development in a pilot study of preterm infants. *Brain Behav* 2016; 6: e00434.
- Lengfeld JE, Lutz SE, Smith JR, Diaconu C, Scott C, Kofman SB, et al. Endothelial Wnt/beta-catenin signaling reduces immune cell infiltration in multiple sclerosis. *Proc Natl Acad Sci USA* 2017; 114: E1168–77.
- Lim SS, Vos T, Flaxman AD, Danaei G, Shibuya K, Adair-Rohani H, et al. A comparative risk assessment of burden of disease and injury attributable to 67 risk factors and risk factor clusters in 21 regions, 1990–2010: a systematic analysis for the Global Burden of Disease Study 2010. *Lancet* 2012; 380: 2224–60.
- Lindstrom K, Lindblad F, Hjern A. Preterm birth and attention-deficit/hyperactivity disorder in schoolchildren. *Pediatrics* 2011; 127: 858–65.
- Lips ES, Cornelisse LN, Toonen RF, Min JL, Hultman CM, International Schizophrenia C, et al. Functional gene group analysis identifies synaptic gene groups as risk factor for schizophrenia. *Mol Psychiatry* 2012; 17: 996–1006.
- Lips ES, Kooyman M, de Leeuw C, Posthuma D. JAG: A computational tool to evaluate the role of gene-sets in complex traits. *Genes* 2015; 6: 238–51.
- Ma B, Hottiger MO. Crosstalk between Wnt/beta-Catenin and NF-kappaB Signaling Pathway during Inflammation. *Front Immunol* 2016; 7: 378.
- Marret S, Mukendi R, Gadisseux JF, Gressens P, Evrard P. Effect of ibotenate on brain development: an excitotoxic mouse model of microgyria and posthypoxic-like lesions. *J Neuropathol Exp Neurol* 1995; 54: 358–70.
- Matcovitch-Natan O, Winter DR, Giladi A, Vargas Aguilar S, Spinrad A, Sarrazin S, et al. Microglia development follows a stepwise program to regulate brain homeostasis. *Science* 2016; 353: aad8670.
- McCarthy KD, de Vellis J. Preparation of separate astroglial and oligodendroglial cell cultures from rat cerebral tissue. *J Cell Biol* 1980; 85: 890–902.
- Melief J, Koning N, Schuurman KG, Van De Garde MD, Smolders J, Hoek RM, et al. Phenotyping primary human microglia: tight regulation of LPS responsiveness. *Glia* 2012; 60: 1506–17.
- Michell-Robinson MA, Touil H, Healy LM, Owen DR, Durafourt BA, Bar-Or A, et al. Roles of microglia in brain development, tissue maintenance and repair. *Brain* 2015; 138 (Pt 5): 1138–59.
- Miron VE, Boyd A, Zhao JW, Yuen TJ, Ruckh JM, Shadrach JL, et al. M2 microglia and macrophages drive oligodendrocyte differentiation during CNS myelination. *Nat Neurosci* 2013; 16: 1211–8.
- Miyamoto A, Wake H, Ishikawa AW, Eto K, Shibata K, Murakoshi H, et al. Microglia contact induces synapse formation in developing somatosensory cortex. *Nat Commun* 2016; 7: 12540.
- Moore T, Hennessy EM, Myles J, Johnson SJ, Draper ES, Costeloe KL, et al. Neurological and developmental outcome in extremely preterm children born in England in 1995 and 2006: the EPICure studies. *BMJ* 2012; 345: e7961.
- Muro S. A DNA Device that Mediates Selective Endosomal Escape and Intracellular Delivery of Drugs and Biologicals. *Adv Funct Mater* 2014; 24: 2899–906.
- NCBI. SNP FAQ Archive [Internet]. Bethesda (MD): National Center for Biotechnology Information (US); 2005-. The dbSNP Mapping Process. 2005. Available from: <https://www.ncbi.nlm.nih.gov/books/NBK44455/> (25 November 2018, date last accessed).
- Nosarti C, Giouroukou E, Healy E, Rifkin L, Walshe M, Reichenberg A, et al. Grey and white matter distribution in very preterm adolescents mediates neurodevelopmental outcome. *Brain* 2008; 131 (Pt 1): 205–17.
- Nosarti C, Nam KW, Walshe M, Murray RM, Cuddy M, Rifkin L, et al. Preterm birth and structural brain alterations in early adulthood. *Neuroimage Clin* 2014; 6: 180–91.
- Oppen-Rhein R, Strimmer K. From correlation to causation networks: a simple approximate learning algorithm and its application to high-dimensional plant gene expression data. *BMC Syst Biol* 2007; 1: 37.
- Pandit AS, Ball G, Edwards AD, Counsell SJ. Diffusion magnetic resonance imaging in preterm brain injury. *Neuroradiology* 2013; 55 (Suppl 2): 65–95.
- Perry VH, Nicoll JA, Holmes C. Microglia in neurodegenerative disease. *Nat Rev Neurol* 2010; 6: 193–201.
- Rangon CM, Schang AL, Van Steenwinckel J, Schwendimann L, Lebon S, Fu T, et al. Myelination induction by a histamine H3 receptor antagonist in a mouse model of preterm white matter injury. *Brain Behav Immun* 2018; 74: 265–76.
- Reyes-Reyes EM, Teng Y, Bates PJ. A new paradigm for aptamer therapeutic AS1411 action: uptake by macropinocytosis and its stimulation by a nucleolin-dependent mechanism. *Cancer Res* 2010; 70: 8617–29.
- Riddle A, Dean J, Buser JR, Gong X, Maire J, Chen K, et al. Histopathological correlates of magnetic resonance imaging-defined chronic perinatal white matter injury. *Ann Neurol* 2011; 70: 493–507.
- Ring DB, Johnson KW, Henriksen EJ, Nuss JM, Goff D, Kinnick TR, et al. Selective glycogen synthase kinase 3 inhibitors potentiate insulin activation of glucose transport and utilization in vitro and in vivo. *Diabetes* 2003; 52: 588–95.
- Rivest S. Regulation of innate immune responses in the brain. *Nat Rev Immunol* 2009; 9: 429–39.
- Robinson EC, Valstar M, Hammers A, Ericsson A, Edwards AD, Rueckert D. Multivariate statistical analysis of whole brain structural networks obtained using probabilistic tractography. *Med Image Computing Comput-Assist Intervent* 2008; 11 (Pt 1): 486–93.
- Schafer J, Strimmer K. An empirical Bayes approach to inferring large-scale gene association networks. *Bioinformatics* 2005; 21: 754–64.
- Schang AL, Van Steenwinckel J, Chevenne D, Alkmark M, Hagberg H, Gressens P, et al. Failure of thyroid hormone treatment to prevent inflammation-induced white matter injury in the immature brain. *Brain Behav Immun* 2014; 37: 95–102.
- Schindelin J, Arganda-Carreras I, Frise E, Kaynig V, Longair M, Pietzsch T, et al. Fiji: an open-source platform for biological-image analysis. *Nat Methods* 2012; 9: 676–82.
- Shah DK, Doyle LW, Anderson PJ, Bear M, Daley AJ, Hunt RW, et al. Adverse neurodevelopment in preterm infants with postnatal sepsis or necrotizing enterocolitis is mediated by white matter abnormalities on magnetic resonance imaging at term. *J Pediatr* 2008; 153: 170–5, 175.e1.
- Shi F, Yap PT, Wu G, Jia H, Gilmore JH, Lin W, et al. Infant brain atlases from neonates to 1- and 2-year-olds. *PLoS One* 2011; 6: e18746.
- Shimizu T, Kagawa T, Wada T, Muroyama Y, Takada S, Ikenaka K. Wnt signaling controls the timing of oligodendrocyte development in the spinal cord. *Dev Biol* 2005; 282: 397–410.
- Shimizu T, Smits R, Ikenaka K. Microglia-induced activation of non-canonical Wnt signaling aggravates neurodegeneration in demyelinating disorders. *Mol Cell Biol* 2016; 36: 2728–41.
- Shiow LR, Favrais G, Schirmer L, Schang AL, Cipriani S, Andres C, et al. Reactive astrocyte COX2-PGE2 production inhibits oligodendrocyte maturation in neonatal white matter injury. *Glia* 2017; 65: 204–37.
- Sieger D, Moritz C, Ziegenhals T, Prykhozhiy S, Peri F. Long-range Ca²⁺ waves transmit brain-damage signals to microglia. *Dev Cell* 2012; 22: 1138–48.
- Smith SM. Fast robust automated brain extraction. *Hum Brain Mapp* 2002; 17: 143–55.
- Smyth GK. Linear models and empirical bayes methods for assessing differential expression in microarray experiments. *Stat Appl Genet Mol Biol* 2004; 3: Article3.
- Sokol SY. Spatial and temporal aspects of Wnt signaling and planar cell polarity during vertebrate embryonic development. *Semin Cell Dev Biol* 2015; 42: 78–85.
- Spittle AJ, Boyd RN, Inder TE, Doyle LW. Predicting motor development in very preterm infants at 12 months' corrected age: the role of

- qualitative magnetic resonance imaging and general movements assessments. *Pediatrics* 2009; 123: 512–7.
- Spittle AJ, Walsh JM, Potter C, McInnes E, Olsen JE, Lee KJ, et al. Neurobehaviour at term-equivalent age and neurodevelopmental outcomes at 2 years in infants born moderate-to-late preterm. *Dev Med Child Neurol* 2017; 59: 207–15.
- Squarzoni P, Oller G, Hoeffel G, Pont-Lezica L, Rostaing P, Low D, et al. Microglia modulate wiring of the embryonic forebrain. *Cell reports* 2014; 8: 1271–9.
- Stolp BH, Fleiss B, Arai Y, Supramaniam V, Vontell R, Birtles S, et al. Interneuron development is disrupted in preterm brains with diffuse white matter injury: observations in mouse and human. *Frontiers in physiology* 2019.
- Subramanian A, Tamayo P, Mootha VK, Mukherjee S, Ebert BL, Gillette MA, et al. Gene set enrichment analysis: a knowledge-based approach for interpreting genome-wide expression profiles. *Proc Natl Acad Sci USA* 2005; 102: 15545–50.
- Supramaniam V, Vontell R, Srinivasan L, Wyatt-Ashmead J, Hagberg H, Rutherford M. Microglia activation in the extremely preterm human brain. *Pediatr Res* 2013; 73: 301–9.
- Thion MS, Ginhoux F, Garel S. Microglia and early brain development: An intimate journey. *Science* 2018; 362: 185–9.
- Tran FH, Zheng JJ. Modulating the wnt signaling pathway with small molecules. *Protein science : a publication of the Protein Society* 2017; 26: 650–61.
- Twilhaar ES, Wade RM, de Kieviet JF, van Goudoever JB, van Elburg RM, Oosterlaan J. Cognitive outcomes of children born extremely or very preterm since the 1990s and associated risk factors a meta-analysis and meta-regression. *JAMA Pediatr* 2018; 172: 361–7.
- van Amerongen R, Mikels A, Nusse R. Alternative wnt signaling is initiated by distinct receptors. *Sci Signal* 2008; 1: re9.
- van der Sar AM, Stockhammer OW, van der Laan C, Spaink HP, Bitter W, Meijer AH. MyD88 innate immune function in a zebrafish embryo infection model. *Infect Immun* 2006; 74: 2436–41.
- van Haastert IC, Groenendaal F, Uiterwaal CS, Termote JU, van der Heide-Jalving M, Eijssermans MJ, et al. Decreasing incidence and severity of cerebral palsy in prematurely born children. *J Pediatr* 2011; 159: 86–91.e1.
- Verdonk F, Roux P, Flamant P, Fiette L, Bozza FA, Simard S, et al. Phenotypic clustering: a novel method for microglial morphology analysis. *J Neuroinflamm* 2016; 13: 153.
- Verney C, Monier A, Fallet-Bianco C, Gressens P. Early microglial colonization of the human forebrain and possible involvement in periventricular white-matter injury of preterm infants. *J Anat* 2010; 217: 436–48.
- Verney C, Pogledic I, Biran V, Adle-Biassette H, Fallet-Bianco C, Gressens P. Microglial reaction in axonal crossroads is a hallmark of noncystic periventricular white matter injury in very preterm infants. *J Neuropathol Exp Neurol* 2012; 71: 251–64.
- Volpe JJ. Brain injury in premature infants: a complex amalgam of destructive and developmental disturbances. *Lancet neurology* 2009a; 8: 110–24.
- Volpe JJ. The encephalopathy of prematurity–brain injury and impaired brain development inextricably intertwined. *Semin Pediatr Neurol* 2009b; 16: 167–78.
- Warde-Farley D, Donaldson SL, Comes O, Zuberi K, Badrawi R, Chao P, et al. The GeneMANIA prediction server: biological network integration for gene prioritization and predicting gene function. *Nucleic Acids Res* 2010; 38(Web Server issue): W214–20.
- Wolf SA, Boddeke HW, Kettenmann H. Microglia in Physiology and Disease. *Annu Rev Physiol* 2017; 79: 619–43.
- Wood NS, Marlow N, Costeloe K, Gibson AT, Wilkinson AR. Neurologic and developmental disability after extremely preterm birth. EPICure Study Group. *N Engl J Med* 2000; 343: 378–84.
- Woodward LJ, Anderson PJ, Austin NC, Howard K, Inder TE. Neonatal MRI to predict neurodevelopmental outcomes in preterm infants. *N Engl J Med* 2006; 355: 685–94.
- Wu HC, Shen CM, Wu YY, Yuh YS, Kua KE. Subclinical histologic chorioamnionitis and related clinical and laboratory parameters in preterm deliveries. *Pediatr Neonatol* 2009; 50: 217–21.
- Yu CH, Nguyen TT, Irvine KM, Sweet MJ, Frazer IH, Blumenthal A. Recombinant Wnt3a and Wnt5a elicit macrophage cytokine production and tolerization to microbial stimulation via Toll-like receptor 4. *Eur J Immunol* 2014; 44: 1480–90.
- Yuen TJ, Silbereis JC, Griveau A, Chang SM, Daneman R, Fancy SP, et al. Oligodendrocyte-encoded HIF function couples postnatal myelination and white matter angiogenesis. *Cell* 2014; 158: 383–96.
- Zhan T, Rindtorff N, Boutros M. Wnt signaling in cancer. *Oncogene* 2017; 36: 1461–73.
- Zhao C, Deng Y, Liu L, Yu K, Zhang L, Wang H, et al. Dual regulatory switch through interactions of Tcf7l2/Tcf4 with stage-specific partners propels oligodendroglial maturation. *Nat Commun* 2016; 7: 10883.